HIGH TEMPERATURE FORMING OF BORONIZED DUPLEX STAINLESS STEEL

ROSNAINI BINTI SAIDAN

FACULTY OF ENGINEERING
UNIVERSITY OF MALAYA
KUALA LUMPUR
2015

HIGH TEMPERATURE FORMING OF BORONIZED DUPLEX STAINLESS STEEL

ROSNAINI BINTI SAIDAN

DISSERTATION SUBMITTED IN FULFILLMENT OF
THE REQUIREMENTS FOR THE DEGREE OF
MASTER OF ENGINEERING SCIENCE

FACULTY OF ENGINEERING
UNIVERSITY OF MALAYA
KUALA LUMPUR

JANUARI 2015

UNIVERSITY OF MALAYA

ORIGINAL LITERARY WORK DECLARATION

Name of Candidate: **ROSNAINI BINTI SAIDAN**
I.C. No.:
Matric No.: **KGA100045**

Name of Degree: **MASTER OF ENGINEERING SCIENCE**

Title of Dissertation ("this Work"):
HIGH TEMPERATURE FORMING OF BORONIZED DUPLEX STAINLESS STEEL

Field of Study: **ADVANCED MATERIALS**

I do solemnly and sincerely declare that:

(1) I am the sole author/write of this Work;
(2) This Work is original;
(3) Any use of any work in which copyright exists was done by way of fair dealing and for permitted purposes and any excerpt or extract from, of reference to or reproduction of any copyright work has been disclosed expressly and sufficiently and the title of the Work and its authorship have been acknowledged in this Work;
(4) I do not have any actual knowledge nor ought I reasonably to know that the making of this work constitutes an infringement of any copyright work;
(5) I hereby assign all and every rights in the copyright to this Work to the University of Malaya ("UM"), who henceforth shall be owner of the copyright in this work prohibited without the written consent of UM having been first had and obtained;
(6) I am fully aware that if in the course of making this Work I have infringed any copyright whether intentionally or otherwise, I may be subject to legal action or any other action as may be determined by UM.

Candidate's Signature Date

Subscribed and solemnly declared before,

Witness's Signature Date

Name:

Designation:

ABSTRACT

The purpose of this work is to study the forming effect of boronized duplex stainless steel (DSS) at high temperature. Pack-boronizing of treated-DSS was carried out at 1223 K for 2, 4 and 6 hours, resulting surface hardness that range between 1890 and 2418 HV. The effects of microstructure, strain rate and surface hardness on high temperature forming process of the boronized treated-DSS were investigated. The forming was also done to its counterpart, the untreated (as-received) DSS, as a controlling factor. The results showed that in general, boronizing increased the flow stress of the forming, as similarly, higher surface hardness also increased the flow stress of the forming. However, the flow stress of the boronized treated-DSS was significantly lower than that of the boronized as-received DSS and comparable to the flow stress of non-boronized as-received DSS, therefore the flow stress during the forming is not only affected by the surface hardness but also strongly affected by the original microstructure of the substrate. The much lower flow stress is attributed to the superplasticity brought about by the fine grain microstructure of the treated-DSS. The study also concluded that with slower strain rate, the surface integration of the boronized treated-DSS can be maintained even though the hardness of the boronized treated DSS is relatively high.

ABSTRAK

Tujuan penyelidikan ini dijalankan adalah untuk mengkaji kesan ubah-bentuk pada suhu tinggi bagi keluli tahan karat dupleks (DSS) yang diboronkan. DSS terawat diboronkan pada suhu 1223 K bagi tempoh 2, 4 dan 6 jam, yang menghasilkan kekerasan permukaan di antara 1890 HV dan 2418 HV. Kesan mikrostruktur, kadar terikan dan kekerasan permukaan bagi proses ubah-bentuk DSS terawat pada suhu tinggi dikaji. Ubah-bentuk DSS asal yang diboronkan juga dilakukan untuk tujuan perbandingan. Hasil kajian menunjukkan secara amnya, pemboronan akan meningkatkan aliran tegasan dalam proses ubah-bentuk. Kekerasan permukaan yang tinggi juga meningkatkan aliran tegasan dalam proses ubah-bentuk. Walaubagaimanapun, aliran tegasan bagi DSS terawat yang diboronkan jelas lebih rendah daripada DSS asal yang diboronkan dan hampir menyamai aliran tegasan DSS asal yang walaupun tidak diboronkan. Ini bermakna, aliran tegasan semasa proses ubah-bentuk bukan hanya kesan daripada kekerasan permukaan tetapi jelas juga disebabkan oleh mikrostruktur bahan tersebut. Tegasan aliran yang rendah ini disebabkan oleh kesuperplastikan yang daripada butir mikrostruktur halus bagi DSS terawat. Kajian ini juga merumuskan dengan merendahkan kadar terikan, keteguhan permukaan bagi DSS terawat yang diboronkan dapat dikekalkan walaupun kekerasannya tinggi.

ACKNOWLEDGEMENTS

Thank you to Allah s.w.t. for giving me the strength and patience to complete my masters study.

I would like to express my gratitude to Dr. Iswadi Jauhari for an opportunity given to me to involve in this research. His supervision, advice and guidance as well as the extraordinary experiences throughout the work are really appreciated. His truly scientist intuition, oasis of ideas and passions in science, exceptionally inspired and enrich my growth as a student and enhance my potential in many areas.

A special thanks to my parents, Saidan Bin Nik and Rubiayah Bt Md Yusof for their love, encouragement and moral support. To my siblings, thanks for being supportive and caring.

I also like to thank everybody especially my friends; my superplastic team (Superplastic Girls), Gojus Q, department staffs, and GGG Girls who are important to the realization of my masters degree.

Last but not least, thank you to Mr. Sharuzzamal, Mr. Firdaus, Farah and PTSBees family for their understanding and courage on my study. As well as expressing my apology that I could not mention personally one by one.

Finally, thank you to HIR (UM.C/625/1/HIR/058) and UM (PV053/2011A) for financing my research project. Apart than that, thank you to the UM RA scheme for supporting my fees. I am grateful in every possible way.

Rosnaini Binti Saidan
Faculty of Engineering, UM
2015

TABLE OF CONTENTS

CHAPTER 4: RESULTS AND DISCUSSIONS

CHAPTER 5: CONCLUSIONS

LIST OF FIGURES

LIST OF TABLES

LIST OF SYMBOLS AND ABBREVIATIONS

Symbols	Explanation
m	Strain-rate sensitivity
σ	Plastic flow stress
F	Applied force
A	Cross-sectional area
K	Constant

Abbreviations	Explanation
DSS	Duplex Stainless Steel
SEM	Scanning Electron Machine
FESEM	Field Emission Scanning Electron Microscope
EDM	Electrical Discharge Machine
XRD	X-ray Diffraction
JIS	Japanese Industrial Standards
GBS	Grain Boundary Sliding
T_m	Melting Temperature
m	High Strain-Rate Sensitivity
FeB	Ferum Boride
Fe_2B	Ferum (II) Boride
CrB	Chromium Boride

CHAPTER 1

INTRODUCTION

1.1 General

Superplasticity is the phenomenon where a material undergoes a very large plastic deformation before failure. Superplastic materials are characterized by their exceptional ductility where an elongation as high as 8000% can be achieved (Carrino *et al.*, 2003). Since this phenomenon offers a lot of industrial potentials, numerous attempts have been made to develop superplasticity in various materials and also to apply the technology in engineering areas.

Boronizing is one of the surface engineering techniques used to harden surface of steel. Boronizing is a thermochemical treatment in which boron atoms are diffused into a metal surface to form hard boride layers with the base material. It was reported that a wide range of materials including ferrous materials, non-ferrous materials and some super alloys can be boronized (Vipin Jain, G. Sundararajan, 2002). The boronizing process can be carried out in solid, liquid or gaseous medium. The most frequently used method is in solid medium or pack boronizing, because of the simplicity of equipment.

Previous studies show that combination of superplasticity phenomenon and boronizing has successfully improved the properties of duplex stainless steel. The results obtained through dual compression method also initiated a new development of high temperature forming through this work (I. Jauhari *et. al*, 2011).

In this study, duplex stainless steel (DSS) is used as the boronized substrate material. Besides characterized by the balance ratio of α-ferrite and γ-austenite, DSS is a material

that can exhibit superplastic behaviour at high temperature. DSS is widely utilized in oil and gas production and transmission, petroleum industries, petro-chemical process plants, shipbuilding, transportations and for pulp and paper production equipments (F. Zucchi *et. al*, 2005 and H. Sieurin, R. Sandstrom, 2005).

Conventionally, devices or parts are initially formed to a specific shape before the boronizing process and not to be exposed to any plastic deformation process after boronizing to avoid surface disintegration. However, for complex-shaped parts, it is difficult to attain a uniform boronizing. Contrary to this conventional process, this research develops deformation process to form parts or devices after boronizing bulk material.

First step of the process is boronizing of duplex stainless steel to achieve a certain degree of hardness and uniform boronized layer. The second step is hot deformation on the boronized DSS at different parameters; surface hardness, type of microstructure and strain rate. Un-boronized DSS was also deformed for comparison purpose.

1.2 Research Objectives

The objectives of this research are:

a) To study the feasibility of superplastic deformation of boronized duplex stainless steel

b) To evaluate properties of forming boronized duplex stainless steel

1.3 Scope of Research

There are two parts in this work which are explained in the next subsections.

1.3.1 Boronizing Process

Pack-boronizing was conducted using a stainless steel container at different boronizing time. Two different types of microstructure; fine and coarse grains were used for comparison purpose. The process was carried out in a tube furnace with controlled atmosphere using argon gas at superplastic temperature. Boronized layer thickness and surface hardness before and after boronizing were evaluated.

1.3.2 Forming Process

Boronized DSS from process in subsection 1.3.1 was used. Forming process at high temperature was performed using compression testing machine that equipped with high-temperature furnace under controlled gas atmosphere. Boronized DSS was deformed without presence of boron powder at different strain rate. Effects of grain microstructure, surface hardness and strain rate were analyzed.

CHAPTER 2

LITERATURE REVIEW

2.1 Superplasticity

In general, superplasticty can be defined as a phenomenon of materials that are able to undergo large uniform strains prior to failure in excess of 200% or more. The current record for elongation in metals which stands at 8000% elongation in commercial bronze is shown in Figure 2.1 (Chandra, 2002). Superplasticity has been observed in several kinds of materials, such as metals (including aluminium, magnesium, iron, titanium and nickel-based alloys), ceramics (including monolitihcs and composites), intermetallics (including iron, nickel, titanium base) and laminates (Xing *et. al*., 2004). There are 2 types of superplasticity which are micrograin or structural superplasticity and internal stress superplasticity (Valiev, 2000).

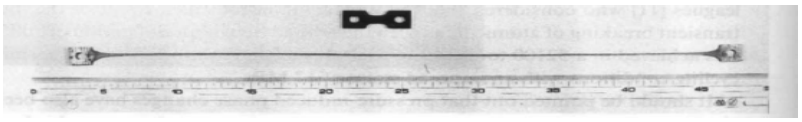

Figure 2.1 A demonstration of superplasticity in Cu–Al alloy (8000% elongation)

It has been reported that superplastic behavior in most metals, alloys and ceramics are associated with three main characteristic stated by Hertzberg (1996)

(1) fine grain size (on the order of 1-10μm)

(2) deformation temperature > 0.5 T_m (where T_m is the absolute melting point)

(3) a strain rate sensitivity factor *m* which is more than 0.3

2.1.1 High Strain Rate Sensitivity

Strain rate sensitivity represents the capacity of the material to resist necking and influences the overall deformation during superplastic deformation (Kirthi, 2007). High strain rate sensitivity allows inhibition of necking, which means no localized of failure at a reduced-cross section area. For superplastic alloys, the characteristic mechanical behavior observed is a strong dependence of flow stress, σ on strain rate, $\dot{\varepsilon}$ at the superplastic temperature. The strain rate sensitivity exponent referred to as *m* provides a measure of the strain rate sensitivity of flow stress and can be defined by the equation below:

$$m = \frac{\partial (\ln \sigma)}{\partial (\ln \dot{\varepsilon})} \qquad (1)$$

It follows that, from expressing the flow stress-strain rate relation by the following equation:

$$\sigma = \frac{F}{A} = K\dot{\varepsilon}^{m} \qquad (2)$$

where F = applied force

A = cross-sectional area

K = constant

$\dot{\varepsilon} = \frac{1dl}{ldt} = -\frac{1}{A}\frac{dA}{dt}$ = strain-rate

m = strain-rate sensitivity factor

Superplastic behavior is usually observed when *m* is greater or equal to 0.4. For most superplastic materials *m* lies within the range of 0.4 to 0.8. Figure 2.2 shows the relation between σ, $\dot{\varepsilon}$ and m.

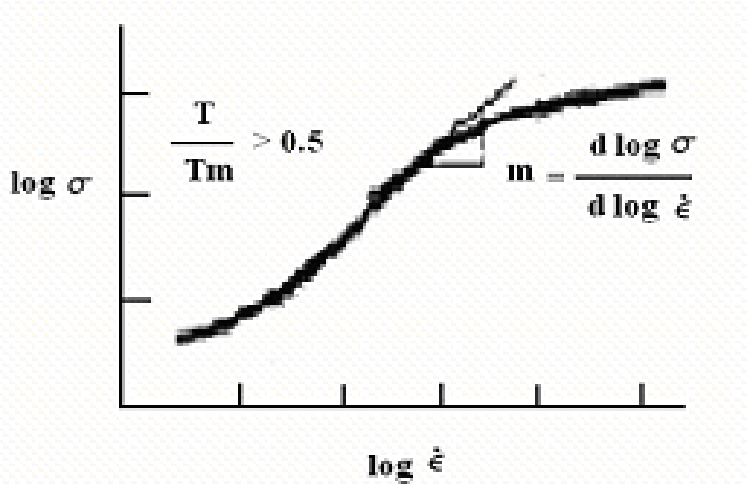

Figure 2.2 Normalized curve of log stress versus log strain

2.1.2 Fine grain size

As mentioned earlier, fine grain size is one of the main characteristic of superplasticity. It has been well understood that ductility of materials increases as the grain size becomes finer. It is critical for the material to have fine grain structure in order to create superplasticity or to deform in the superplastic condition. Figure 2.3 illustrates that decreasing grain size has an effect on widening the superplastic region. Metals with fine grain microstructure sized within the range of 1- 10 μm tends to exhibit superplasticity at the temperature of deformation.

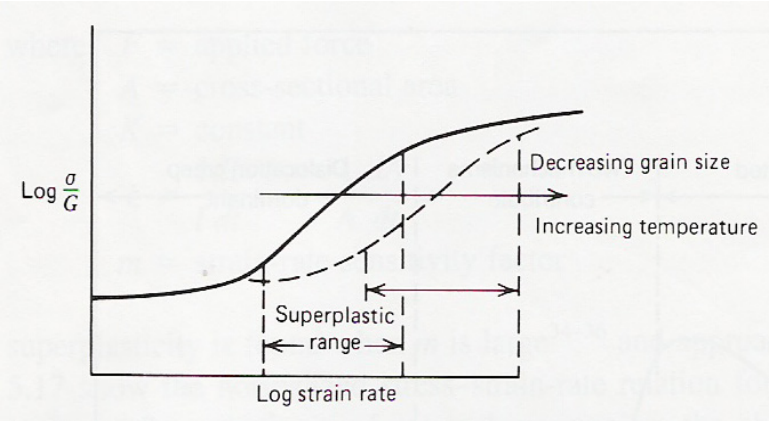

Figure 2.3 Effect of decreasing grain size on the range of superplastic region

2.1.3 Temperature

Temperature is considered to be one of the most important parameters in superplastic deformation since temperature is closely related with superplastic deformation and the movement of matter in general. Superplasticity is considered as the movement of matter such as gas particles, solid particles and water particle. The movement of matter is a temperature-dependent mechanism.

Superplasticity in most materials commonly occurs at elevated temperature. The optimal temperature of superplastic forming is higher than 0.5 T_m where T_m is the melting point of material expressed in Kelvin.

2.1.4 Mechanism of Superplasticity

Several metallurgical factors have been proposed to explain superplastic behavior. Superplasticity results in high ductility through grain boundary sliding and fine equiaxed microstructure. Grains are observed to change their neighbours and seen to emerge at the free surface from the interior (Chandra, 2002). The particular structural condition is that the material is of very fine grain size and the presence of a two-phase structure is usually of importance in maintaining this fine grain size during testing. Furthermore, the strain rate of superplastic deformation depends strongly on the grain size of the materials and temperature.

Several models of mechanisms have been proposed for superplastic deformation (Langdon, 1970; Mukherjee, 1971; Gifkins, 1976; Arieli and Mukherjee, 1980). Recent studies using high voltage transmission electron microscope (TEM) support the idea that grain boundary sliding is the primary mechanism (Chandra, 2000). Figure 2.4 shows the microstructure movement during superplastic deformation. In superplastic deformation

however, strain in a given direction is due to the motion of individual grains or clusters of grains relative to each other by sliding and rolling. During deformation, the grains remain equiaxed or become equiaxed. Although there is some difference in grain shape during the accommodation, the grain shape and size remain identical before and after deformation.

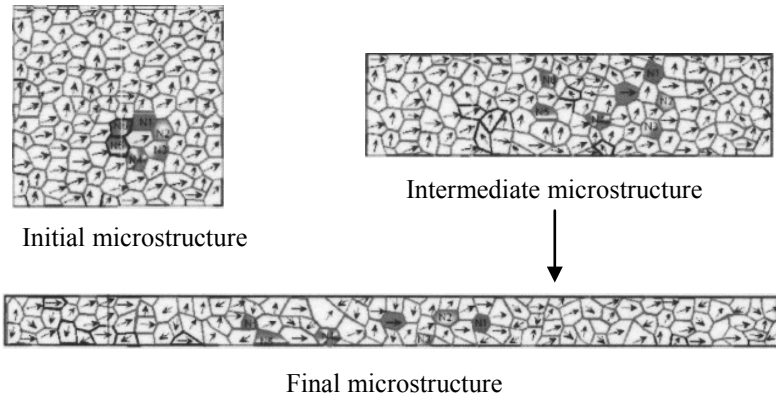

Figure 2.4 Evolution of microstructure during superplastic deformation (Chandra, 2002)

The accommodation mechanisms can be divided into three general groups (Mukherjee, 2002): (a) diffusional accommodation, (b) accommodation by dislocation motion and (c) combined model with elements of dislocation and diffusional accommodation.

Diffusional accommodation occurs when the mass flow is due to the diffusion process in the vicinity of grain boundary. When a load is applied to a material, the deformation is due to grain boundary diffusion and sliding, as a result of strain. The process is indicated in Figure 2.5.

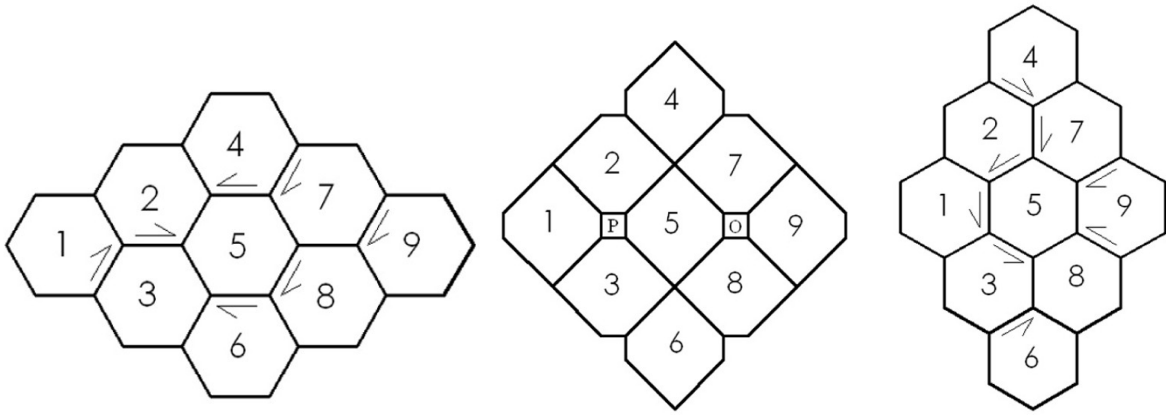

Figure 2.5 The process of diffusional accommodation (Zelin and Mukherjee, 1996)

For accommodation by dislocation motion, it can be understood by dividing the grain into two parts; the core inside the grain and mantle at the grain boundary, as shown in Figure 2.6 (a). In order for the grain to slide, initially the dislocations which move onto the grain boundary are accumulated at the triple point of grain boundary. From there, the dislocations move into the mantle due to stress concentration. Finally, the dislocations motion inside the mantle results in the grain rotation. Figure 2.6 (b) shows the process of accommodation by dislocation motion. The accommodation which combines dislocation and diffusional processes are shown in Figure 2.7.

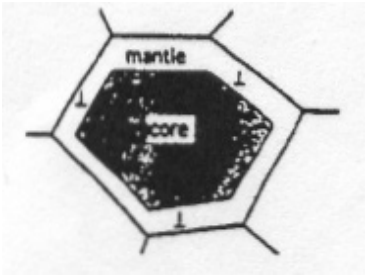

(a)

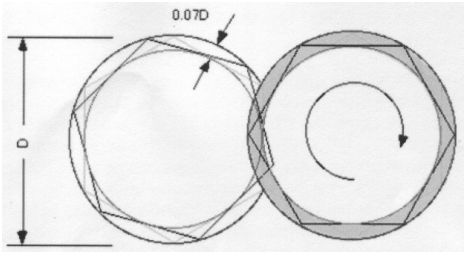

(b)

Figure 2.6 (a) The core inside the grain and mantle is at the grain boundary (b) Dislocation motion inside the mantle results in the grain rotation (D = diameter). (Zelin and Mukherjee,

1996)

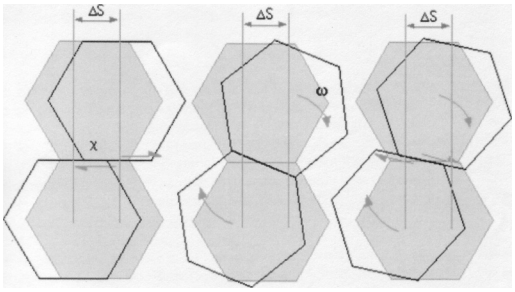

Figure 2.7 The accommodation which combines dislocation and diffusional processes

2.1.5 Applications of Superplasticity

Superplasticity has been developed and implemented through several application processes. There are two major processes in using superplasticity for commercial applications. The first is superplastic forming (SPF) which utilizes large deformability of the superplastic material and the other is superplastic diffusion bonding (SPDB) where good bonding is achieved on the bonding interface as a result of local superplastic flow (Kum *et. al*, 1984: Walser *et. al*, 1985).

Superplasticity is mostly being used to form parts in aerospace applications (Xing *et al.,* 2004, 1988: Tsuzuka *et al.,* 1991) but nowadays there are also some non-aerospace applications as well. In aerospace applications, superplastic forming is increasingly being used to form very complex geometries. Nickel-based alloys are used to form turbine discs with integral blades while aluminium alloys are fabricated to form low-weight and high-stiffness airframe control surfaces. Small-scale structural elements are also produced by utilizing the SPF process (Xing *et al*., 2004). Meanwhile, non-aerospace applications using aluminium alloys include containers with complex surface profiles, decorative panels for internal and external cladding of buildings and also high speed train (Superplastic

aluminium forming, 1988).

Superplastic forming is usually conducted at high temperatures and under controlled strain rate. This process is typically obtained with a single-sided die where the sheet is heated at a high temperature and gas pressure is applied in order to push the sheet into the tool (Friedman and Luckey, 2004). Due to the normally low die costs and relatively slow forming rates, this process is usually found to be economically viable for small to moderate production quantities (Bloor *et al*., 1994). Also, the simplicity of the dies and the fact that only a single configuration die is suitable often permit a short lead time to produce parts once the design is completed. Figure 2.8 (a) illustrates the SPF process and figure 2.8 (b) shows an example of a gas turbine rotor with integral blades produced by the SPF process.

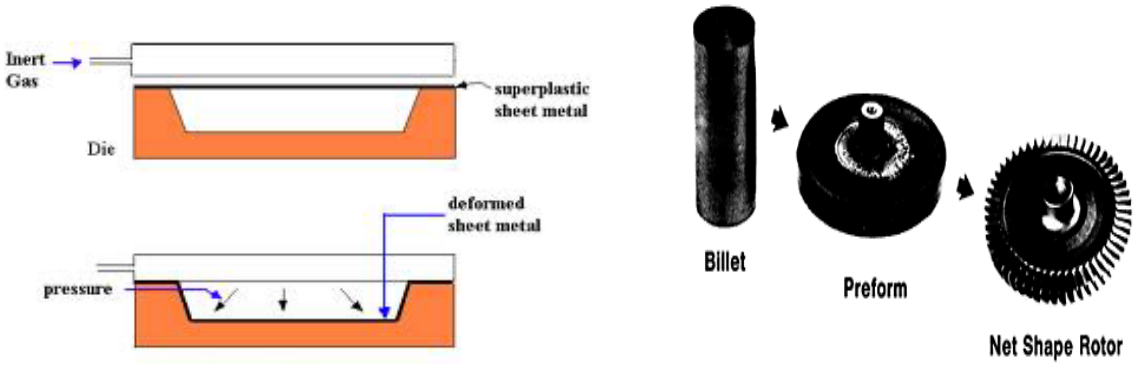

(a) (b)

Figure 2.8 (a) Superplastic forming(SPF) process (Internet Reference-1) and (b) uperplastic forming of a superalloy gas-turbine rotor with integral blades (Internet Reference-2)

Superplasticity also plays an important role in the solid state diffusion bonding (DB) process. It has been reported that superplastic deformation accelerates the solid state diffusion the bonding process while obtaining an effective bonding (high strength) with minimum material deformation (Jauhari *et al.,* 2002). The acceleration of solid state joining

by superplastic deformation is closely related to the development of grain boundary sliding in the material (Lutfulin *et. al*., 1995). These processes permit fabrication of parts with local thickness variations, attachments and complex sandwich structures (Bloor *et at*., 1994). SPF together with DB has been implemented to produce hollow engine blades, fan and compressor blades for aero engines (Xun and Tan, 2000; Xing *et. al*., 2004).

2.2 Boronizing

Boronizing has been widely used to improve the surface properties of metals. Nowadays, boronizing is being successfully applied to ferrous and non-ferrous alloys (Balokhonov *et al*, 2000; Hoffmann *et al,2001*). The boride layer produced through boronizing have high hardness, good wear resistance and high corrosion and oxidation resistance (C.H. Xu *et al*, 1997). With hardness produced exceeding 2000 HV, this process promises a better resistance to friction and abrasion compared to carburizing and nitriding (Sinha, 1991; Meric *et al.*, 2000).

The boronizing process can be carried out in a solid, liquid or gaseous medium. Among these methods, boronizing is mostly carried out by the solid or pack-medium method due to its simplicity and cost-effectiveness (Keddam and Chentouf, 2005). In the boronizing process, boron is diffused into the surface layer of metal. Boron is usually derived from a solid, gaseous or liquid substance which is in contact with the metal surface. Chemical reaction is not involved directly with the metal but may be catalyzed by the presence of the metal.

As mentioned in a previous section, although liquid and gas boronizing are usually used nowadays, solid or pack boronizing still remains as a process that is the most simple, economical, original and industrially reliable.

Pack boronizing is a process in which boron is derived from a solid compound that decomposes at the metal surface. This process consists of packing the work piece in a container containing a solid boronizing agent (boronizing powder) and heating it slowly in a furnace to attain a temperature of about 1173 K to 1223 K. To avoid complications, boronizing should be carried out in a protective gas atmosphere, which may be pure argon, pure nitrogen or a mixture of hydrogen and either argon or nitrogen.

The containers used for pack boronizing are usually made from heat resistant steels which is most economical in the long run. To avoid unevenly boronized parts, the use of smaller containers is generally preferred for a more uniform effect on the boronized components.

In pack-boronizing, temperature and time are the main control factors. The thickness of boride layer is determined by the temperature and time of the treatment (Jain and Sundararajan, 2002). The boron amount determines how much it can be diffused and the temperature determines the depth of boron penetration for a set of holding time. In general, the boron atoms diffused lead to formation of a thicker boronized layer. In order to produce a certain degree of boronizing and boronized thickness layer, it is very crucial to select the suitable parameters. The easiest way to obtain thicker boronized layer is by increasing the temperature. However, there is a temperature limitation due to thermal shock in cooling and it is imperative to maintain the fine microstructure of the work piece.

2.3 Duplex Stainless Steel

Duplex Stainless Steel (DSS) contain between 18 to 25% chromium, 4 to 7% nickel and up to 4% molybdenum and is water quenched from a hot working temperature that is between 1000 and 1050^{o}C to produce a microstructure that is approximately half ferrite and half austenite (Kohser *et al.* , 2003). The nickel content is insufficient to generate a fully austenitic structure and the result of the combination of ferritic and austenitic structure is called duplex.

The duplex stainless steel, as its name implies, are defined as a family of stainless steel which consists of a two phase aggregated microstructure of α-ferrite and γ-austenite. The microstructure of the standard duplex stainless steel that consist both ferritic and austenitic structures is shown in Figure 2.9. It combines the attractive properties of austenitic and ferritic stainless steel: high tensile strength and fatigue strength, good toughness even at low temperatures, adequate formability and weldability and excellent resistance to stress corrosion cracking, pitting and general corrosion (Cabrera *et al*., 2003). These factors promote DSS as an alternative to austenitic stainless steels.

With reference to Figure 2.10, duplex stainless steel initially solidifies as ferrite, then transforms to a matrix of ferrite and austenite on further cooling. In order to avoid formation of brittle intermetalic phases, the usable temperature range of duplex stainless steel is restricted to the range of 223 K to 553 K (Hasan, 2005).

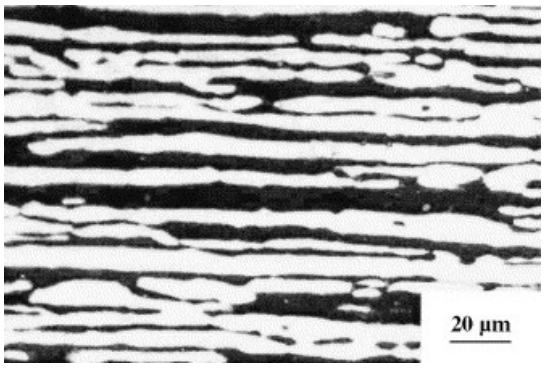

Figure 2.9 Near equal amount of austenite (light etched regions) and ferrite (dark etched regions) microstructure of duplex stainless steel (Muthupandi et al, 2005).

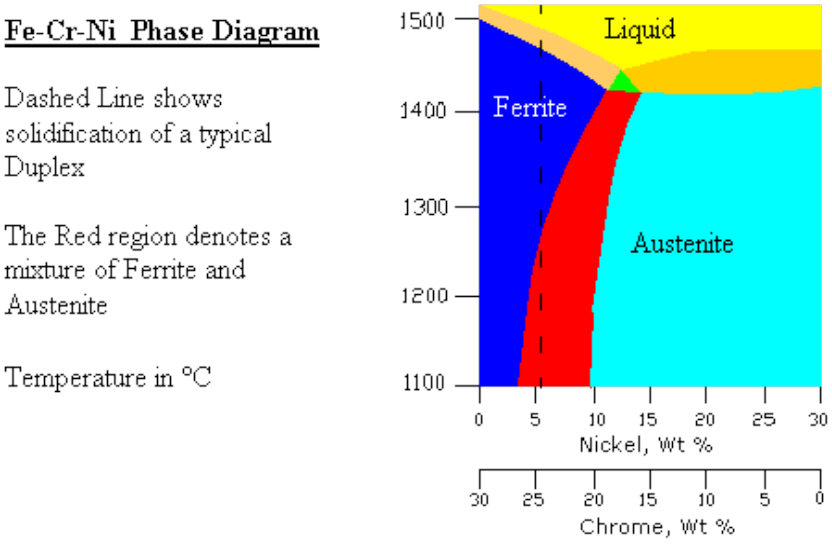

Figure 2.10 Fe-Cr-Ni phase diagram (Internet Reference-3)

Superplasticity in duplex stainless steel has been investigated for over 3 decades. The term "superplastic duplex stainless steel" was first used in 1980. Han and Hoong (1999) reported that duplex stainless steel with fine grain microstructure has the ability to show superplastic behavior since the grain growth is effectively suppressed at high temperature due to the two phase aggregated microstructure. One of the earliest investigation works of superplasticity in duplex stainless steel reported by Hayden *et al.* in 1967 showed 500%

elongation in 25Cr-6.5Ni-0.6Ti hot-rolled duplex stainless steels.

Since a fine-grained microstructure is the most important feature of superplastic materials, it is known that the processing step in producing the finest microstructures which are stable at the deformation temperature and would enhance superplasticity is definitely important. Several distinct thermo-mechanical processing techniques have been used to develop a superplastic microstructure in duplex stainless steels. One example is thermo-mechanical process which consists of hot-rolling the material in the temperature range of 1100–1300°C followed by cold-rolling with 50% reduction (Jimenez *et al*, 2001). The fine grain duplex microstructure is obtained through precipitation of the second phase particles when the thermo-mechanically treated duplex stainless steel is heated up at test temperature (Han and Hong, 1999). Figure 2.11 shows the microstructure of thermo-mechanically treated duplex stainless steel with grain sizes of about 10 μm after it has been heated, up at test temperature ranging from 850 to 1100°C.

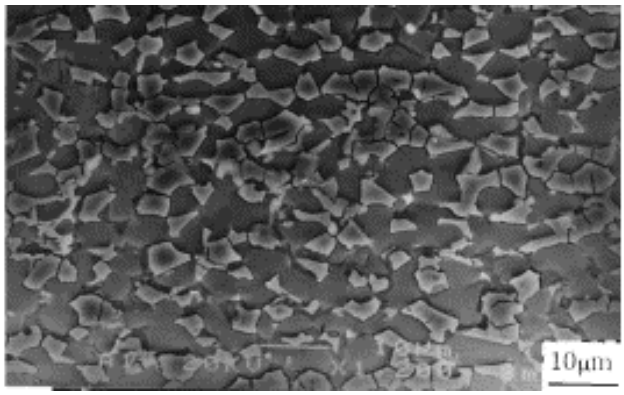

Figure 2.11 Microstructure of fine grain duplex stainless steel (Miyamoto *et al*., 2001)

It has been reported by Jimenez *et al.* (2001) that the microstructure evolution during deformation identifies grain boundary sliding as the mechanism responsible for superplastic deformation of duplex stainless steels. On the other hand, some previous studies suggest that the dynamic recrystallization of the softer phase in duplex stainless steel or other duplex microstructure, which occurs continuously during deformation, could be the dominant mechanism for superplasticity at temperatures in the range 800–191100°C. However, Tsuzaki *et al*. (1996) suggested that grain boundary sliding is the dominant mechanism for superplasticity in duplex stainless steel, and the role of dynamic recrystallization is to keep the grain size fine, suitable for grain boundary sliding. Furthermore, the study conducted by Han and Hong (1999) also concluded that the grain boundary sliding assisted by dynamic recrystallization is considered to be the controlling mechanism for superplastic deformation of DSS.

Based on the previous studies on dual compression method by I. Jauhari *et. al* (2011), the present work is developed in order to study the feasibility of high temperature forming behaviour of DSS. The characteristics of superplasticity on duplex stainless steel are exploited through forming process. Extra attention was given to observations made on superplastic effect and surface integrity of the substrate during the forming process. The results gathered therein shall then become the reference for the employment of plastic deformation process after boronizing or generally after surface hardening processes.

CHAPTER 3

EXPERIMENTAL PROCEDURE

3.1 Substrate Material

Duplex stainless steel (DSS) compared to Japanese Industrial Standards (JIS SUS329J1) was used as the substrate material in this study. The chemical composition of the DSS is shown in Table 3.1.

Table 3.1 Chemical composition of duplex stainless steel (JIS SUS329J1) in wt %

C	0.06
Si	0.42
Mn	0.30
P	0.03
S	0.06
Ni	4.18
Cr	24.5
Mo	0.49
Fe	Balance

In this study, DSS with two different microstructures are used; (a) coarse microstructure (as-received DSS) and (b) fine microstructure (heat-treated DSS). In order to obtain fine microstructure, the as-received DSS were initially solution treated for 1 hour at 1573K followed by water quenching. The solution treated DSS was then cold-rolled to a plate through a reduction area of 75%. The schematic diagram of the thermo-mechanical treatment of DSS is shown in Figure 3.1. The thermo-mechanically treated alloy showed a superplastic elongation of 1050% at temperature of 1223 K and strain rate of 1×10^{-3} s^{-1} condition (Ogiyama *et al*., 2001).

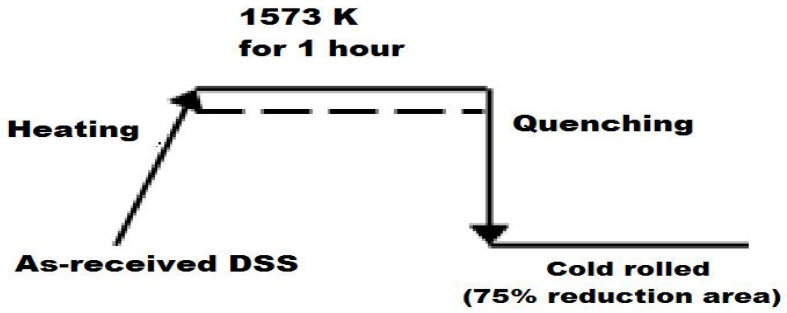

Figure 3.1 Flow chart of the thermo-mechanical treatment process of DSS

3.2 Material Preparation

Both as-received DSS and treated DSS were cut (dash lines) into dimension of 10 mm × 10 mm × 8 mm using EDM wire cut. The dimension of the specimen is shown in Figure 3.2.

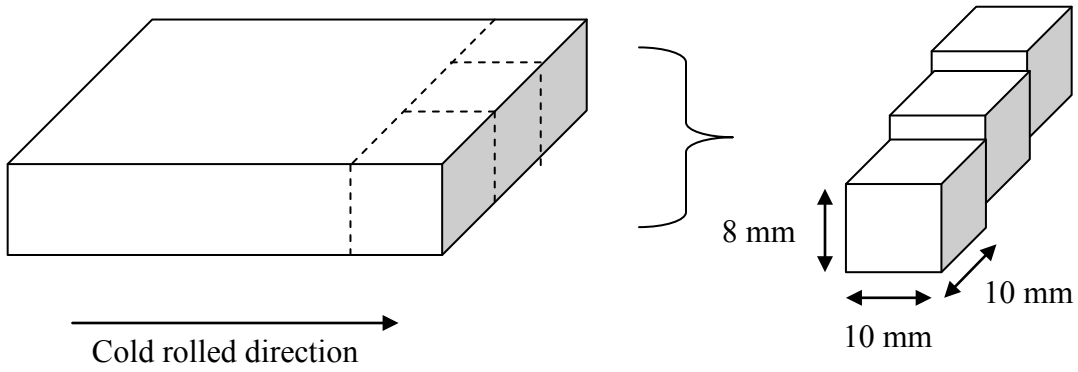

Figure 3.2 Dimension of the cutting specimen of DSS

3.2.1 Grinding and Polishing

The grinding process is one of important operation in material preparation in order to remove any irregularities and eliminate the effects of sectioning. Prior to the boronizing process, the whole surface of specimen is ground using emery paper up to 240-grit which

produces a surface roughness, Ra of 0.3μm (Hanis Ayuni, 2010). After the grinding process, the specimen was washed using ethanol solution to remove contaminants.

3.2.2 Microstructure Evaluation

For microstructure evaluation, the cross-sectioned specimen was ground using emery paper starting with the coarsest, 100-grit to the finest, 1200-grit to remove the oxide layers. Polishing was performed in order to remove scratches and deformation from grinding and to achieve a surface that is highly reflective, flat and defect free. The specimen was polished until a mirror-like surface was obtained. A special etchant for duplex stainless steel was prepared from hydrochloric acid (HCl) saturated with ferric chloride ($FeCl_3$) activated with a small amount of nitric acid (HNO_3), based on the proportion as mentioned by Voort (1984). The polished surface of the specimen was soaked in the etchant solution for few seconds and then washed with distilled water.

3.3 Fabrication of Jigs and Dies

3.3.1 Container for the Boronizing Process

A stainless steel container was designed to conduct the conventional boronizing process. Since boronizing is performed at high temperature, a container made from stainless steel was used due to its high melting point which is between 1673 K and 1723 K. Besides that, it is also known to have corrosion resistance qualities, high ductility, strength and hardness. These properties are very suitable for the conventional boronizing process.

The dimension of stainless the steel container is shown in Figure 3.3. A stainless steel hollow cylinder with an inner diameter of 55 mm was used to fabricate the stainless steel container while a stainless steel solid rod was used to fabricate the removable top and

bottom cover. The solid rod was cut in a similar dimension to size of the inner diameter of the hollow rod for it to be inserted as the bottom cover of the container. The bottom cover was then welded to the container to ensure that it would not come off during the experimental procedure. The removable top cover was also fabricated from a solid rod of 5 mm thickness. Figure 3.4 shows the fabricated stainless steel container.

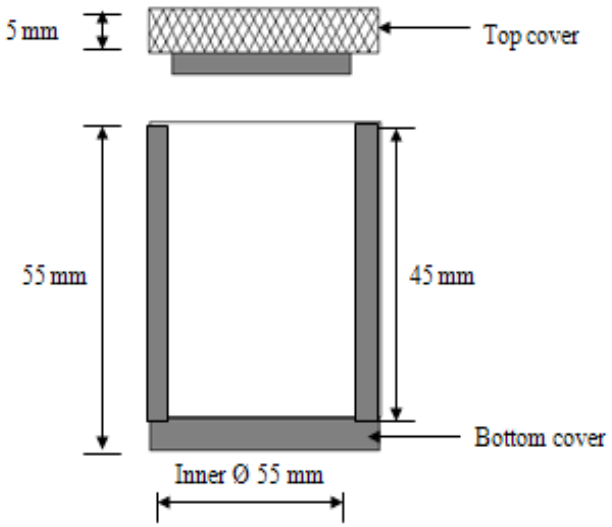

Figure 3.3 Schematic diagram of conventional boronizing container

Figure 3.4 Fabricated conventional boronizing container

3.3.2 Jigs and Dies for Forming Process

Specially designed jigs and dies were fabricated for superplastic deformation process. High temperature resistance stainless steel was used for the fabrication of jigs and dies. The upper temperature limit in the oxidation atmosphere is about 1273 K. The drawing of jigs and dies is shown in Figure 3.5 (a), (b) and Figure 3.6 respectively. These jigs and dies were set up for the forming process which is explained in section 3.5.

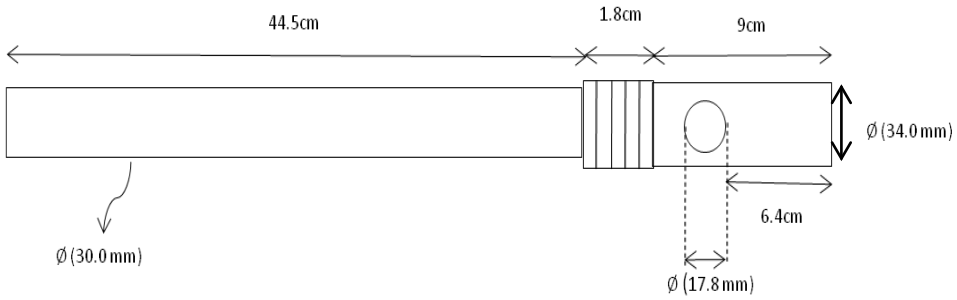

(a) Drawing dimension of upper jig

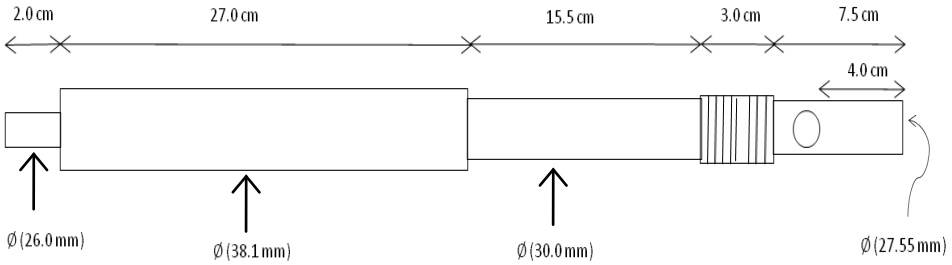

(b) Drawing dimension lower jig

Figure 3.5 Drawing dimension of lower and upper jigs that used for deformation process

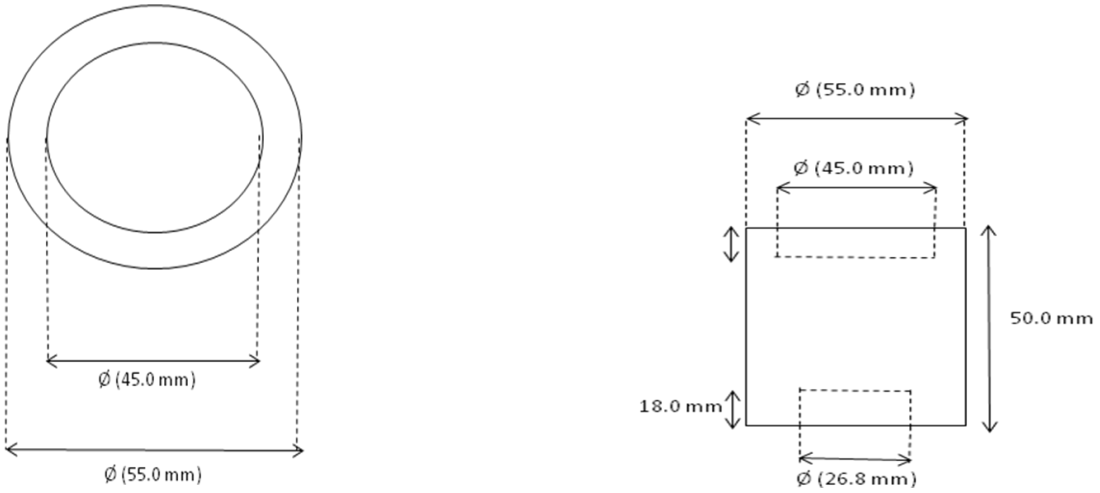

(a) Top View (b) Side View

Figure 3.6 Dimension of dies from (a) top and (b) side views

3.4 Boronizing Process

In this work, pack-boronizing process was carried out. The specimen was surrounded and packed with boron powder in the fabricated stainless steel container as shown in Figure 3.7. Ekabor-1© boron powder was used as the boronizing agent in this process. The container was tapped to make sure it was densely packed and also to prevent air trap.

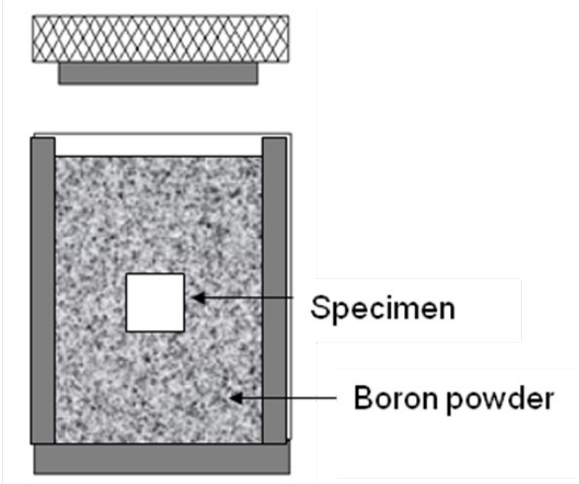

Figure 3.7 Schematic diagram of pack-boronizing set up inside the conventional boronizing container

Boronizing process was carried out at a temperature of 1223 K for 2, 4 and 6 hours holding time in a tube furnace (Carbolite, type CTF 17/75/300) with controlled atmospheric conditions using argon gas. Besides a offering a controlled atmospheric, Argon gas was supplied to prevent oxidation at high temperature. After boronizing process completed, the sample was allowed to cool in the furnace to room temperature. Figure 3.8 shows the flow diagram for the boronizing process.

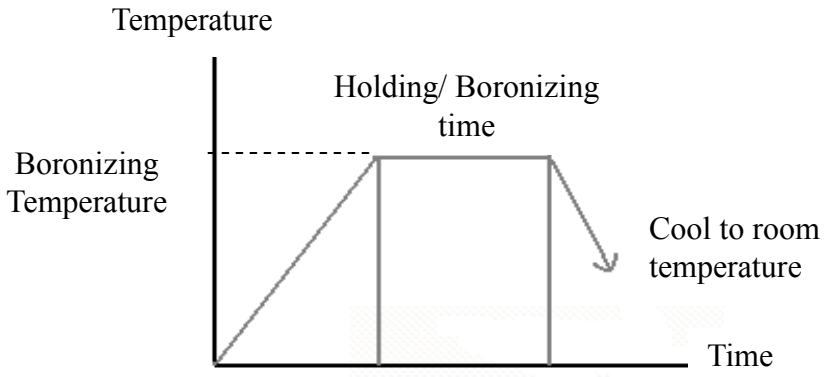

Figure 3.8 Flow diagram of boronizing process

3.5 Forming Process

Superplastic forming was carried out on the boronized specimen using a compression testing machine (Instron) equipped with high-temperature furnace. The specimen was compressed into a fabricated designed die. The sample was put in the die on the end of lower jig. Both upper (movable crosshead) and lower jigs (fixed crosshead) were placed in their specific positions located in the furnace. The picture and cross-section diagram of the compression testing machine for the forming process set up is shown in Figure 3.9.

The forming process was conducted at temperature of 1223 K. The specimen was held for an hour at that temperature to ensure that the specimen reached a homogeneous condition. The specimen was compressed under a selected strain rate of; 1×10^{-3}, 1×10^{-4}, 2×10^{-4} and 6×10^{-5} s^{-1} and strain of 0.4. Once the forming process ended, the specimen was furnace-cooled to room temperature.

(a) Compression testing machine

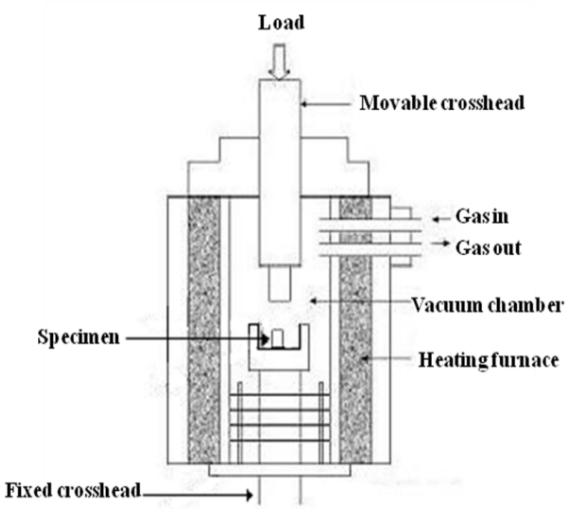

(b) Schematic diagram of forming process set up

Figure 3.9 Picture of Instron compression machine (a) and schematic diagram of experimental apparatus (b) for forming process

For comparison purposes, unboronized as-received and heat-treated DSSs were also deformed. Table 3.2 summarized the experimental conditions of both boronizing and forming processes in this work.

Table 3.2 Summary of experimental conditions for deformation process

Sample	Type of sample		Boronizing Process	Superplastic Forming		
	Treated DSS	As-received DSS	Time (h)	Strain Rate (s^{-1})	Strain (mm/mm)	Deformation time (s)
A-Treated-2hr	/		2	$1x10^{-4}$	0.4	4000
B-Treated-4hr	/		4	$1x10^{-4}$	0.4	4000
C-Treated-6hr	/		6	$1x10^{-4}$	0.4	4000
D-As-received-6hr		/	6	$1x10^{-4}$	0.4	4000
E-Treated-6hr-1 $\times10^{-3}$	/		6	$1x10^{-3}$	0.4	400
F-Treated-6hr-2$\times10^{-4}$	/		6	$2x10^{-4}$	0.4	2000
G-Treated-6hr-6 $\times$ 10^{-5}	/		6	$6x10^{-5}$	0.4	6666
H-Treated-6hrs*-1 $\times10^{-4}$	/		*	$1x10^{-4}$	0.4	4000
I-As-received-6hrs*-1 $\times10^{-4}$		/	*	$1x10^{-4}$	0.4	4000

***** These samples, were exposed to heating at the same temperature for 6 hours without boron powder

3.6 Characterization Methods

Several characterizations and analysis were performed in this study. X-ray diffraction analysis (XRD) was carried out to confirm the presence of boride phases of boronized DSS. The boronized layer was analyzed using an optical microscope and a scanning electron microscope (SEM). The surface hardness of the specimen before and after the boronizing process was measured using microhardness Vickers.

3.6.1 X-ray Diffraction Analysis (XRD)

X-ray diffraction (XRD) is a non-destructive technique to identify the crystalline phases present in solid materials and powders and for analyzing structural properties (such as stress, grain size, phase composition, crystal orientation, and defects) of the phases. The XRD result patterns are like fingerprints of the material that is being examined.

In this study, chemical elements of the specimen, before and after the boronizing process were confirmed using a Philips X'Pert MPD PW3040 XRD with CuKα radiation at 1.54056 Å X-ray wavelength as shown in Figure 3.10. The specimen was scanned from 10° to 80° for 2θ angle at a step size of 0.020 and at a count time for 1.5 s at each step. The surface of the specimen to be characterized by XRD analysis was cleaned with alcohol and placed onto a glass slide.

Figure 3.10 X-Ray Diffraction analysis machine

3.6.2 Optical Microscopy

Morphology analysis can be made using the optical microscope for phase identification. Visual examination enables material surface treatment to be identified and characterized. In a reflected light microscope, the specimen is illuminated by frontal lighting, which is accomplished by means of a small plain-glass reflector placed inside the tube of the microscope (Zainul, 2004).

An optical microscope model Zeiss Axiotech with maximum 1000 times enlargement was connected by a Panasonic digital camera model WV-CP410 to an image analyzer. An MSQ software version 6.5 was used in this study as depicted in Figure 3.11. The optical microscope was used in the microstructural analysis and measurement of boronized layer thickness. The specimen was prepared and ground using various grades of emery paper and polished until a mirror-like surface was achieved. The surface of the specimen was then etched using a special etchant. Excess etchant is washed away with distilled water and the specimen dried with a blower. The specimen was then ready to be observed under a microscope using different magnifications.

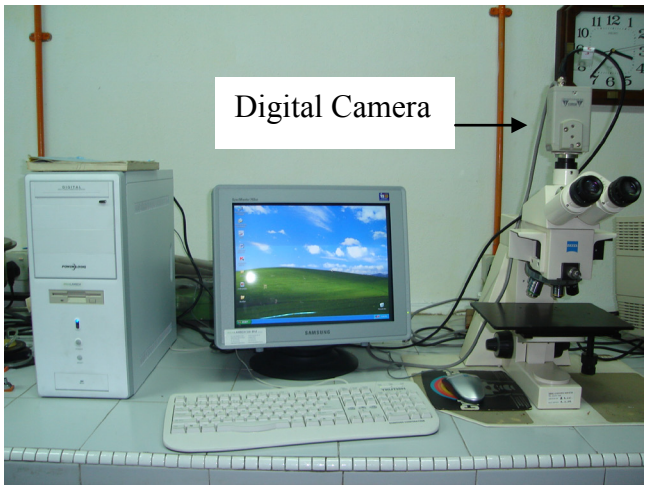

Figure 3.11 Optical microscope model Zeiss Axiotech with connected digital camera and image analyzer.

3.6.3 Scanning Electron Microscopy

With similar functions to that of an optical microscope, the scanning electron microscope is used for deeper analytical microscopy because of its versatility and the wide range of information it can provide. The SEM uses a focused beam instead of light for the specimen imaging and obtains information on its structure and composition. The focused

beam of high-energy electrons is scanned over the surface of a material and interacts with the material, causing a variety of signals—secondary electrons (SE), backscattered electrons (BSE), X-rays, photons, etc.— that may be used to characterize a material with respect to specific properties. The signals are used to modulate the brightness on a display CRT, thereby providing a high-resolution map of the selected material property.

In this study, Philips XL40 SEM as shown in Figure 3.13 was used to capture images of specimen microstructure before and after the boronizing process. A conductive sample is required for analyzing. For a non-conductive sample, generally specimens would be coated using magnetic sputtering of gold. A sample preparation for SEM analysis is similar to an optical microscope analysis. The sample to be analyzed was ground, polished and etched to reveal its morphology. The sample was then put on the stub and placed in the SEM chamber as shown in Figure 3.13.

Figure 3.12 Scanning electron microscope (SEM)

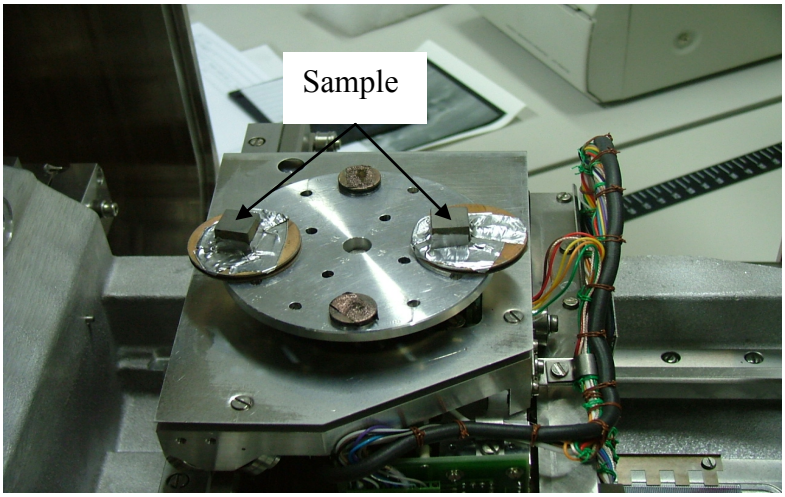

Figure 3.13 Microscope chamber of the SEM where the samples are placed for analysis

3.6.4 Microhardness Tester

According to Metals Handbook, hardness is defined as "Resistance of metal to plastic deformation, usually by indentation". It is the property of a metal-the ability to resist being permanently, deformed (bent, broken, or having its shape changed), when load is applied. The greater the hardness of the metal, the greater resistance it has to deformation.

In this study, hardness measurements were taken at the surface and the cross-section of the boronized sample specimen using. A Vickers hardness test with a diamond indenter test method was used. A load of 2N was applied and then the hardness reading was obtained automatically after measuring the size of indentation. Mitutuyo microhardness tester model MVK-H2 for the hardness test is shown in Figure 3.14.

Figure 3.14 Mitutuyo microhardness tester model MVK-H2

CHAPTER 4

RESULTS AND DISCUSSIONS

4.1 Substrate Material

In this study two types of duplex stainless steel (DSS) were used; as-received DSS with coarse microstructure and treated-DSS with fine microstructure. The optical microstructure images of as-received DSS and thermo-mechanically treated DSS are shown in Figure 4.1 (a) and (b) respectively. The fine microstructure DSS with an average grain size less than 10 μm was obtained during reheating the specimen at the boronizing process at temperature of 1223 K. DSS with fine grain microstructure has the ability to show superplastic behavior at high temperature.

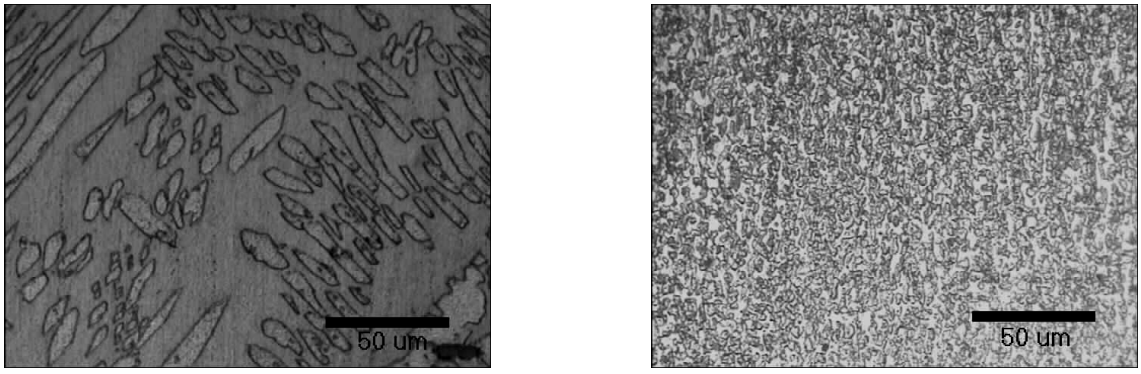

(a) (b)

Figure 4.1 Optical microscope images of (a) thermo-mechanically treated and (b) as-received DSS

The initial hardness of the as-received DSS with coarse microstructure before boronizing was 328 HV. For the treated DSS with fine microstructure, the DSS surface hardness was 420 HV. The increase in hardness for the fine microstructure was due to cold working effect during the thermo-mechanically treatment where the strain hardening

occurred within the grains. Table 4.1 tabulates the characterizations of as-received DSS (non-superplastic material) and treated-DSS (superplastic material).

Table 4.1 Characterization of as-received and treated DSSs

Characterization	As-received DSS	Treated DSS
Grain shape	Elongated	Equiaxed
Grain size	-	~3 μm
Hardness	328 HV	420 HV

4.2 Boronizing Process of DSS

In this step, treated-DSS was boronized at temperature of 1223 K for 2, 4 and 6 hours while as-received DSS was boronized for 6 hours for comparison. XRD analysis was conducted for confirming the occurrence of boronizing process. Morphology analysis and hardness test were also performed for detail characterization.

4.2.1 X-ray Diffraction Analysis (XRD)

The presence of boride phases on the surface of the boronized specimen were confirmed by XRD analysis. Figure 4.2 demonstrates the XRD pattern of the as-received and treated-DSS before and after boronizing for 6 hours at 1223 K. From the figure, the presence of boride phases of FeB, Fe_2B and CrB were detected on the surface of the boronized specimen after boronizing. This results confirmed the successful occurrence of boronizing process of the specimen. Further analysis of XRD is beyond the scope in this study.

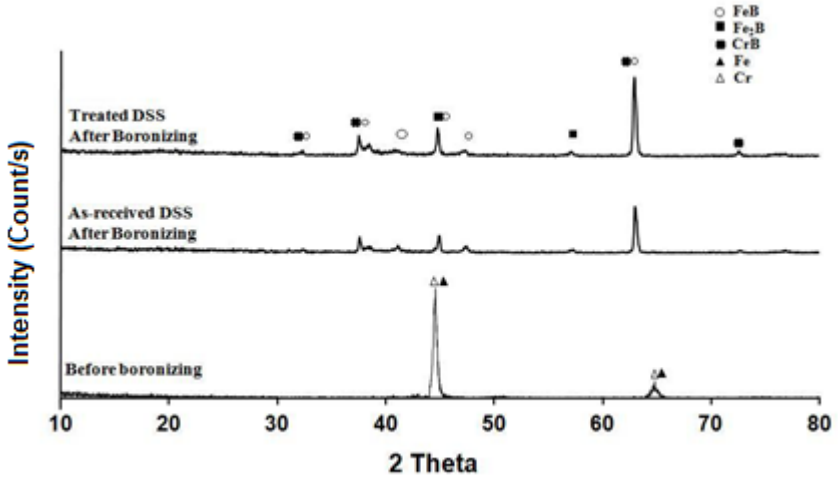

Figure 4.2 X-ray diffraction pattern of as-received and treated-DSSs before and after boronizing at 1223K for 6 hours

4.2.2 Boronized Layer Characterization

Figure 4.3 (a), (b) and (c) shows the optical images of the cross-sectional for boronized treated DSS at 2, 4 and 6 hours respectively. Meanwhile, Figure 4 (d) shows the cross-sectional image of boronized as-received DSS for 6 hours. Both types of microstructures were boronized at 1223 K. A uniform, dense and smooth boronized layer was formed at all the boronized specimens. The compact and smooth morphology is seen due to the presence of alloying elements in DSS. Alloying elements especially chromium and nickel modify coating-substrate interface by changing the diffusivity of boron atoms (Ozbek *et al.*, 2002)

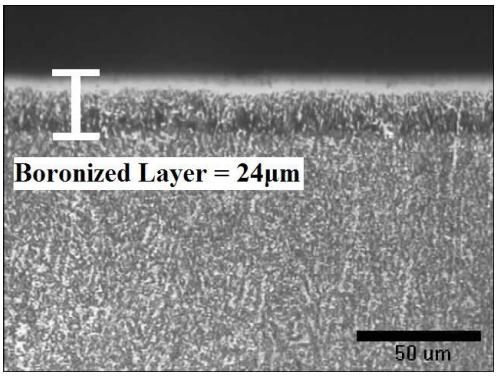

(a) A

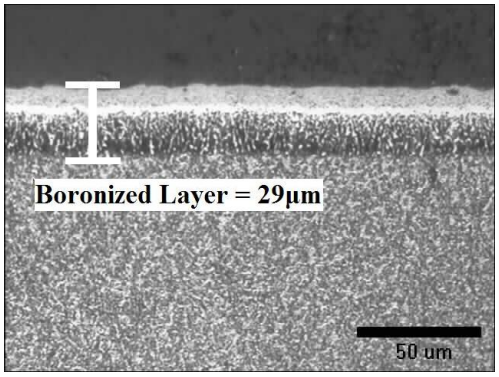

(b) B (Treated-4hr)

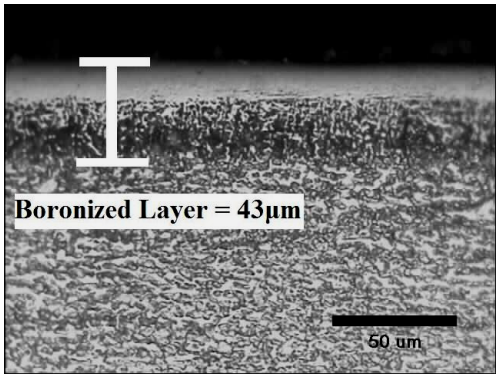

(c) C (Treated-6hr)

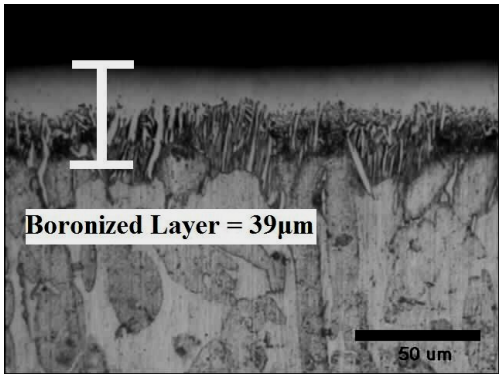

(d) D (As-received-6hr)

Figure 4.3 Cross-section of all boronized DSS at 1223 K for 6 hours

Table 4.2 tabulates the boronized layer thickness and surface hardness obtained for different type of microstructures at different boronizing time. The boronized layer thickness as labelled in previous figure for treated-DSS was in the range of 24 to 43 µm depending on the boronizing time and for as-received DSS was an average of 39 µm. Figure 4.4 shows the plotted layer thickness for these samples.

Table 4.2 Boronized layer thickness of treated and as-received DSSs at different time

Sample	Type of microstructure		Boronizing Time (hour)	Layer thickness (µm)	Surface Hardness (HV)
	Treated-DSS (Fine Grain)	As-received DSS (Coarse grain)			
A (Treated-2hr)	/		2	24	1890
B (Treated-4hr)	/		4	29	2103
C (Treated-6hr)	/		6	43	2418
D (As-received-6hr)		/	6	39	2130

The initial hardness of treated-DSS was 420 HV. Depending on boronizing time, the surface hardness of boronized treated-DSS increased in the range between 1890 and 2418 HV. As-received DSS resulted surface hardness of 2130 HV from 328 HV after boronizing process. Surface hardness profile of boronizing specimens is shown in Figure 4.5.

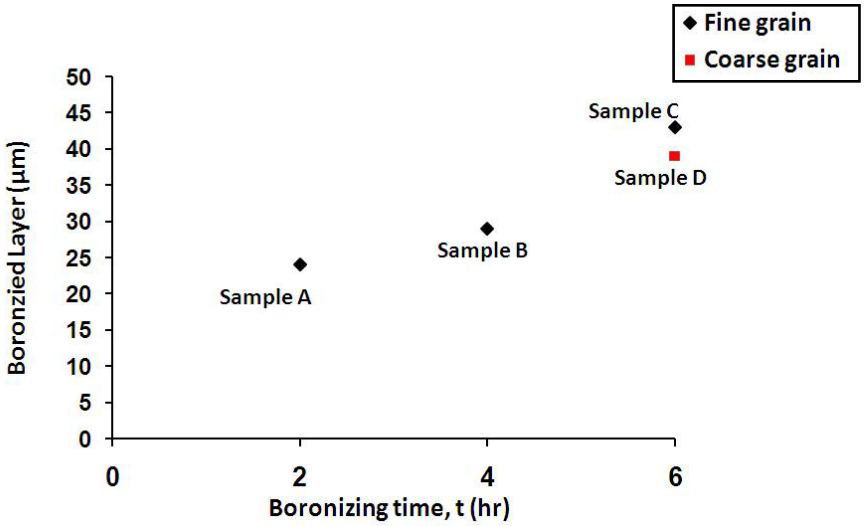

Figure 4.4 Boronized layer thicknesses for different boronizing time and type of microstructure

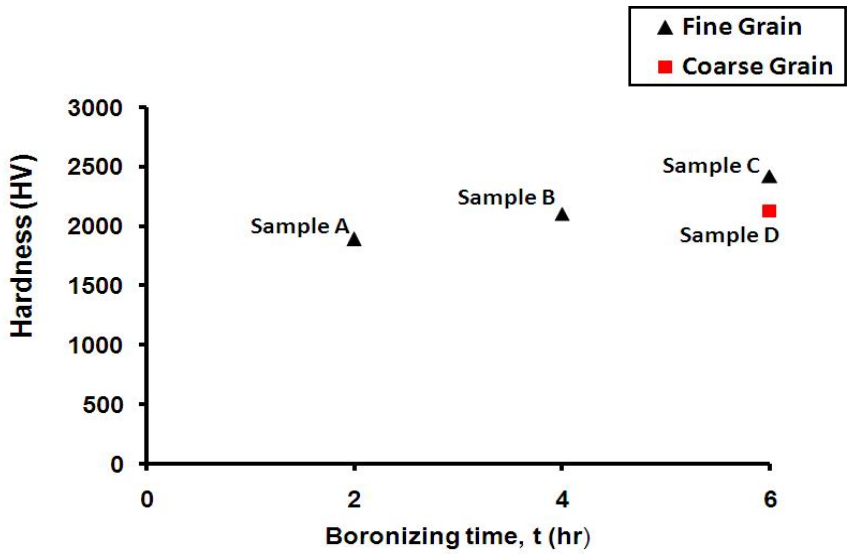

Figure 4.5 Graph of boronized layer thicknesses for different boronizing time and type of microstructure

The microhardness of cross-sectional specimen was also measured from the surface to the substrate. The cross-sectional hardness images of all boronized samples are shown in Figure 4.6. Similar pattern of hardness from the surface into the core was notified for all boronized samples**.** The decrease of hardness towards the core confirming the hardening effect through boronizing process. As the amount of boron atoms available at the surface were higher, therefore the tendency of atoms diffusion and formation boride phases (verified by XRD analysis previously) were higher at the surface as compared to the core.

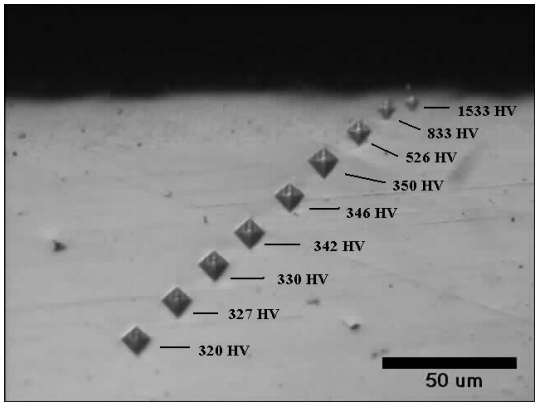

(a) Sample A (Treated-2hr)

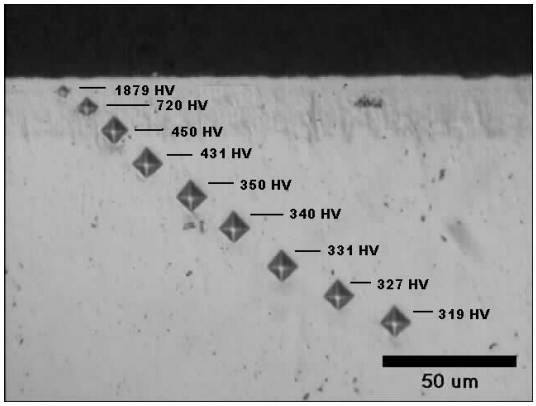

(b) Sample B (Treated-4hr)

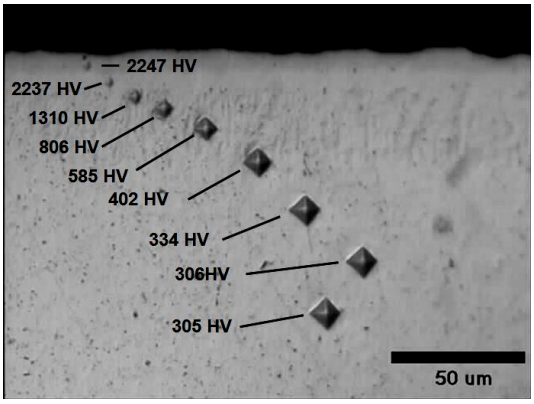

(c) Sample C (Treated-6hr)

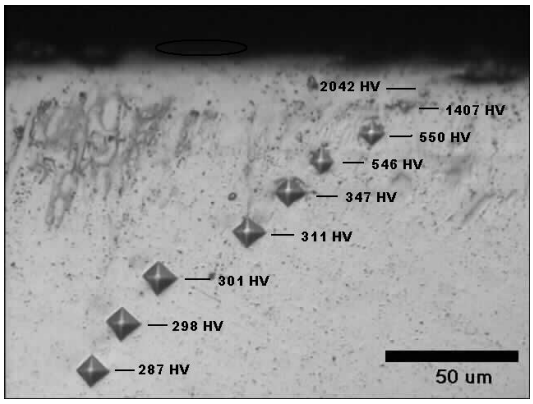

(d) Sample D (As-received-6hr)

Figure 4.6 Microhardness of cross-sectional DSS, boronized at 1223 K for different hours and different types of microstructure

The microhardness for boronized treated-DSS (Sample A, B and C) and boronized as-received DSS (Sample D) from the surface towards the core were profiled in Figure 4.7. For treated-DSS samples that boronized at different time, the profile revealed that longer boronizing time promotes harder surface and thicker boronized layer. As boronizing time increase, it allows more boron atoms to diffuse into the substrate. It was also noted that both treated-DSS (Sample C) and as-received DSS (Sample D) which experienced the same boronizing time duration produced 2418 HV and 2130 HV of surface hardness respectively. The treated-DSS with fine grain having higher value of grain boundaries. Grain boundaries are the most active area in microstructure and the diffusional of boron atoms would be

more active in this area. Therefore, higher value of surface hardness was obtained for treated-DSS sample compared to as-received DSS.

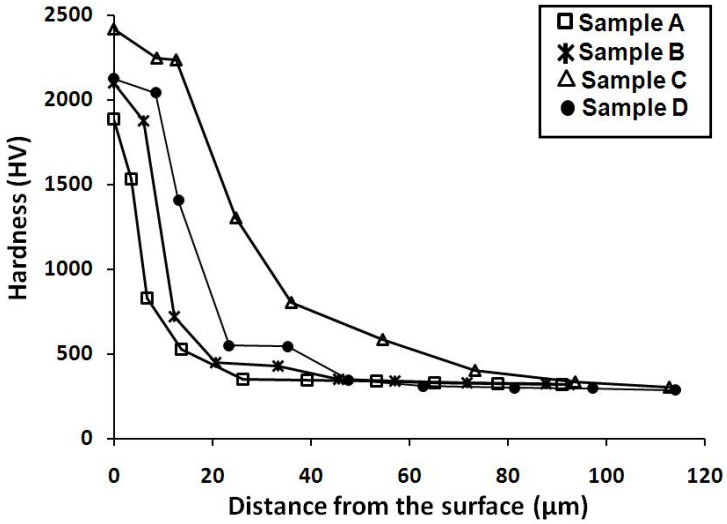

Figure 4.7 Microhardness gradient profile of all boronized samples; A (Treated-2hr), B (Treated-4hr), C (Treated-6hr) and D (As-received-6hr)

4.3 Forming Process

Heat forming of superplastic material; boronized treated-DSS was performed and also for non-superplastic material; boronized as-received DSS were also performed for comparison. Sample was deformed without the presence of boron powder. All boronized samples were compressed at different conditions. From here, effect of different types of grain microstructure, surface hardness and strain rate on the surface integrity of the deformed boronized DSS were analyzed.

4.3.1 Grain Microstructure Effect on Flow Stress

Table 4.3 tabulates the effects of different microstructure and process condition on flow stress. Boronized (Sample C and Sample D) and un-boronized (Sample H and Sample I) specimens for both types of microstructure were deformed at the strain rate of $1x10^{-4}$ s^{-1} and strain of 0.4.

Table 4.3 Forming process conditions of boronized and un-boronized samples for treated-DSS and as-received DSS

ample	Type of sample		Boronizing Process	Forming Process
	Treated DSS	As-received DSS	Time (h)	Flow Stress (MPa)
C (Treated-6hr)	/		6	68
D (As-received-6hr)		/	6	110
H (Treated-6hrs-Unboron)	/		*	20
I (As-received-6hrs-Unboron)		/	*	37

* These samples were exposed to heating at the same temperature for 6 hours without boron powder

The stress-strain relationship for both boronized and un-boronized samples were shown in Figure 4.8. The flow stress for as-received DSS (Sample I) and the treated-DSS (Sample H) were about 37 MPa and 20 MPa respectively. The flow stress of as-received DSS was higher than the treated one. After being boronized, the flow stress of both samples increases remarkably to about 110 and 68 MPa respectively.

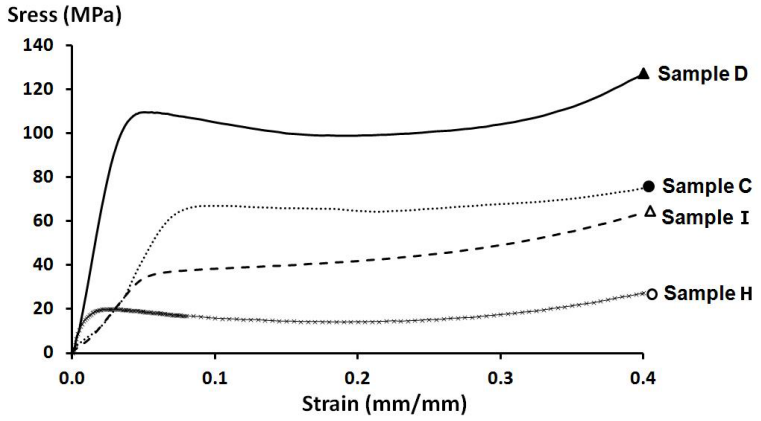

Figure 4.8 Stress-strain relationship of forming boronized samples; C (Treated-6hr) and D (As-received-6hr) and un-boronized samples; H (Treated-6hrs-Unboron) and I (As-received-DSS-6hrs-Unboron)

Apparently, the presence of hard boronized layer increased the flow stress of the samples. Similar trend of results were also reported for case-hardened (B. Hoffmann, 2001). However, for Sample C (2418 HV) and sample D (2130 HV) it interesting to note that the flow stress was not only depend on the hardness of the boronized layer. It was known that the flow stress of Sample C (boronized treated-DSS) was lower than Sample D (boronized as-received DSS) although having higher hardness. Sample C which having fine grain microstructure is suggested affects the flow stress produced. When a load is applied to the specimen which having fine grain microstructure, the deformation is due to grain boundary diffusion and sliding, as a result of strain (Mohd Yusof H.A, 2010). Therefore, although surface hardness of Sample C was higher than Sample D, the occurrence of fine grain of boundary sliding was suggested to produce lower flow stress.

4.3.2 Surface Hardness Effect on Flow Stress

Table 4.4 shows the experimental conditions for this part. Treated-DSS that was boronized at different time were superplastically deformed at strain rate $1x10^{-4}$ s^{-1} and strain of 0.4.

Table 4.4 Forming process at strain rate $1x10^{-4}$ s^{-1} and strain of 0.4 of treated-DSS boronized for different time

Sample	Boronizing Process	Forming Process
	Time (h)	Flow Stress (MPa)
A	2	47
B	4	55
C	6	68

The flow stress of these samples was plotted in Figure 4.9. From the figure, the flow stress decreases as surface hardness decreases. It interesting to observe through Sample A and Sample I which mentioned previously. The flow stress of Sample A was 47 MPa, slightly higher as compared to sample I with flow stress of 37 MPa. Although being boronized and produced surface hardness of 1890 HV, the flow stress of Sample A (treated-DSS) seems comparable to the flow stress of unboronized Sample I (as-received DSS) with surface hardness of 328 HV. This result proved that the fine grain microstructure affected the flow stress. Grain boundary sliding which is the main mechanism for superplastic deformation had probably played the role of producing low flow stress. In addition, fine grain size and deformation temperature are also the main factor of superplastic behaviour.

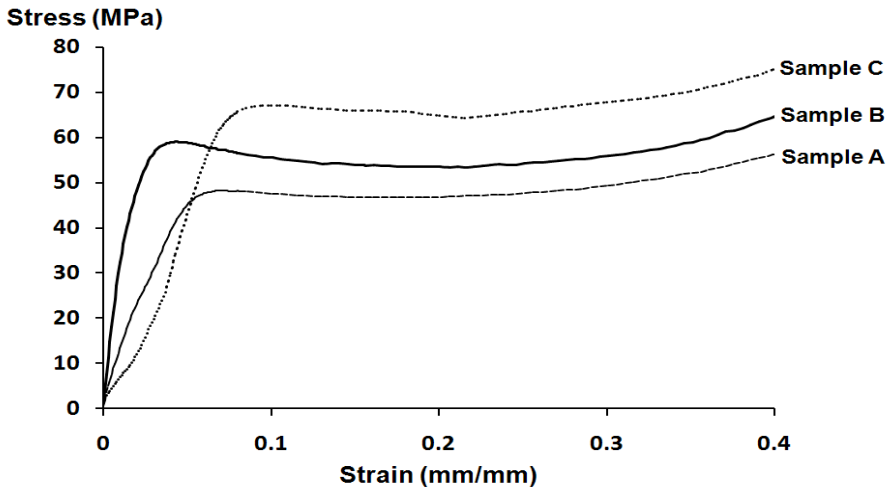

Figure 4.9 Flow stress of forming at temperature of 1223 K for boronized treated-DSS; Sample A (Treated-2hr), Sample B (Treated-4hr) and Sample C (Treated-6hr)

4.3.2.1 Near-surface Microstructure: Effect of Surface Hardness and Grain Microstructure

Near-surface microstructures of boronized treated-DSS (Sample A, Sample B and Sample C) and as-received DSS (Sample D) after forming process is shown in Figure 4.10. All these samples were deformed at strain rate of 1×10^{-4} s^{-1} and strain 0.4. Among the four samples, Sample A (boronized treated DSS) has the lowest hardness and produced the lowest flow stress. Contrary to Sample D (boronized as-received DSS), it has the highest flow stress which has been explained in section 4.3.1. For different hardness samples; Sample A, Sample B and Sample C, the near-surface morphology was similar to the samples' morphology before forming process especially for Sample A and Sample B. It can be seen that although Sample D was boronized at the same duration time as Sample C, the near-surface microstructure of Sample D (as-received DSS) was almost damaged until the core while only a few micro-cracks were observed in Sample C (treated-DSS) . From these results, it showed that hard boronized treated-DSS able to withstand the load applied during deformation process and produced lower flow stress as compared to the boronized

as-received DSS. The fine grain microstructure of treated-DSS probably the factor to withstand the applied load. As reported by Xu *et.* al *(*1996) that the smaller the grain size, the more grain boundaries area and the higher the resistance is to crack propagation.

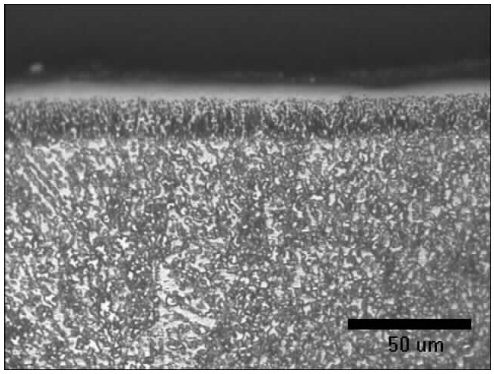

(a) Sample A (Treated-2hr)

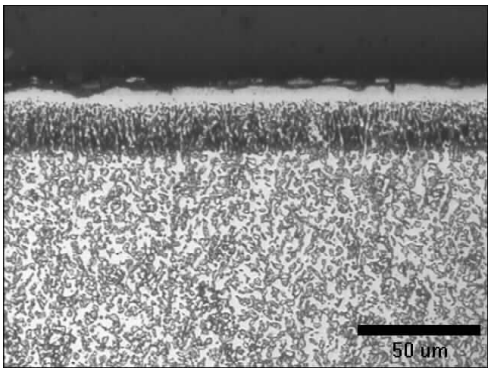

(b) Sample B (Treated-4hr)

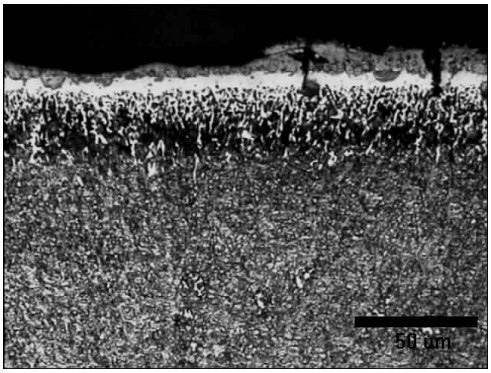

(c) Sample C (Treated-6hr)

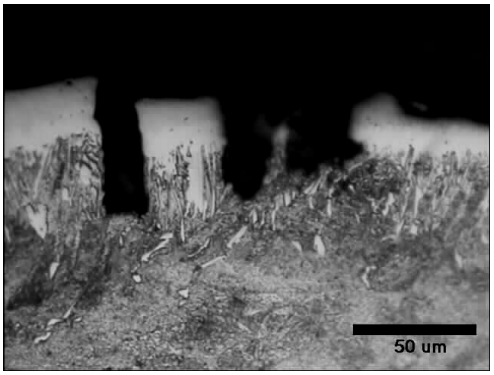

(d) Sample D (As-received-6hr)

Figure 4.10 Cross-sectional images of deformed boronized treated DSS and boronized as-received at strain rate of 1×10^{-4} s^{-1} for strain 0.4 at temperature 1223 K

4.3.3 Strain rate Effect on Flow Stress

Superplastic forming was performed for treated DSS that boronized at 1223 K for 6 hours. The specimen was deformed at strain rate of $1x10^{-4}$ s^{-1} (Sample C), 1×10^{-3} s^{-1} (Sample E), 2×10^{-4} s^{-1} (Sample F), and 6×10^{-5} s^{-1} (Sample G) for strain of 0.4. Table 4.5 tabulates the forming process of these conditions.

Table 4.5 Superplastic forming of treated DSS boronized for 6 hours at different strain rate

Sample	Forming Process			
	Strain Rate (s^{-1})	Strain (mm/mm)	Deformation time (s)	Flow Stress (MPa)
C	$1x10^{-4}$	0.4	4000	68
E	$1x10^{-3}$	0.4	400	140
F	$2x10^{-4}$	0.4	2000	87
G	$6x10^{-5}$	0.4	6666	55

4.3.3.1 High Strain Rate Sensitivity (m value)

In order to prove the superplastic deformation effect in the forming of boronized treated-DSS, the strain rate sensitivity (m value) of the deformation was determined. The flow stress was plotted for each strain rate based on the following equation,

$$\sigma = K\dot{\varepsilon}^{m}$$

where σ is the stress, K the material constant, ἑ the strain rate and *m* is an exponent which known as the strain rate sensitivity. The m value was determined through the data in Table 4.5. Figure 4.11 shows the natural logarithmic plot of σ versus ἑ and demonstrates the value of m=0.3. Most superplastic materials have *m* value typically between 0.3 and 0.8.

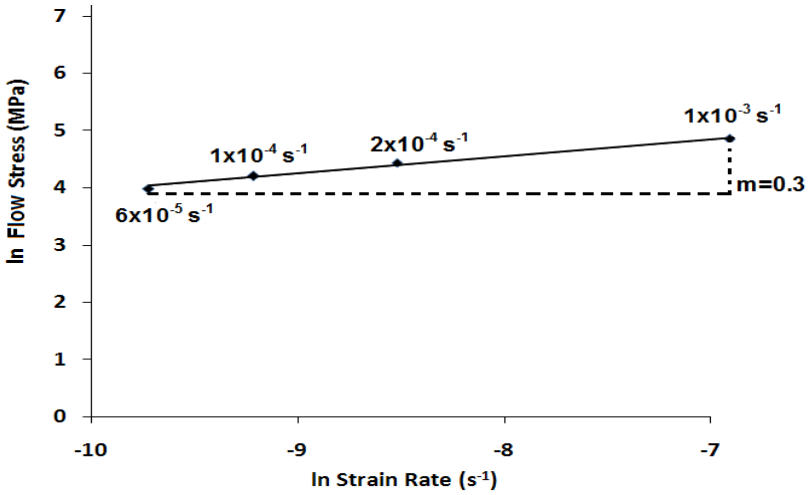

Figure 4.11 Strain rate sensitivity (m) for superplastic forming at different strain rate; $1x10^{-4}$ s^{-1} (Sample C), 1×10^{-3} s^{-1} (Sample E), 2×10^{-4} s^{-1} (Sample F), and 6×10^{-5} s^{-1} (Sample G)

In Figure 4.12, forming at high strain rate resulted flow stress of about 140 MPa (Sample E). At a fixed temperature, as strain rate decreased, the flow stress was also decreased. The flow stress of lower strain rate were 87, 68, 55 MPa for Sample F, Sample C and Sample G respectively. Generally, increasing strain rate leads to the augmentation of flow stress. The results here suggested that the boronizing would hardened the substrate surface and therefore increase during high temperature forming. It also suggests that the flow stress of the surface-hardened substrate could be reduced through superplasticity.

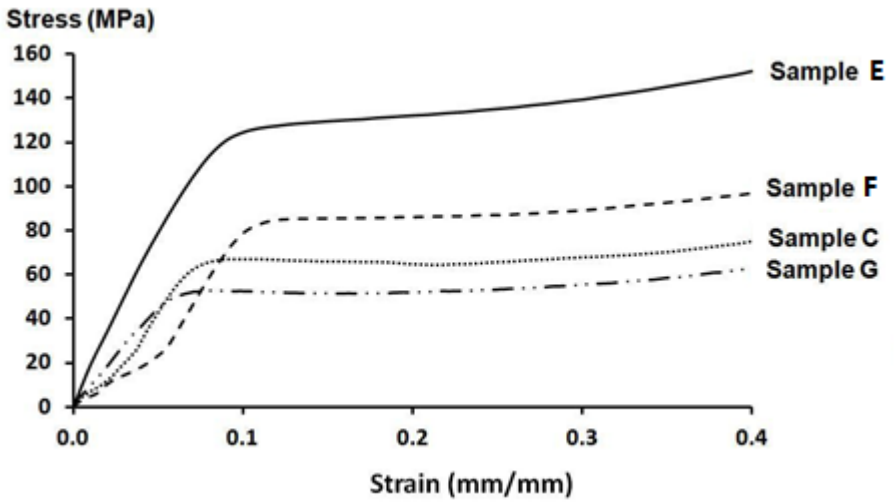

Figure 4.12 Stress-strain relationship for boronized treated DSS deformed at $1x10^{-4}$ s^{-1} (Sample C), 1×10^{-3} s^{-1} (Sample E), 2×10^{-4} s^{-1} (Sample F), and 6×10^{-5} s^{-1} (Sample G)

4.3.3.2 Near-surface Microstructure: Effect of Strain Rate

In this part with reference to Figure 4.12 previously, superplastic forming was done on boronized treated-DSS that boronized for 6 hours. FESEM images in Figure 4.13 shows the near-surface microstructure of boronized treated-DSS after forming at 1223 K and strain rate of 0.4 for different strain rate;1×10^{-3} s^{-1} (Sample E), 2×10^{-4} s^{-1} (Sample F) and 6×10^{-5} s^{-1} (Sample G). With reference to Figure 4.12 previously, forming at the highest strain rate produced high flow stress. From the FESEM images, it showed that at highest strain rate leads to disintegration of boronized layer (Figure 4.13(a)). At the lower strain rate, the flow stress produced was 87 MPa (Figure 4.13 (b)) and surface disintegration was noticed through the microcracks formations into the substrate. In Figure 4.13 (c) there is no sign of surface disintegration after deformation process.

(a) Sample E (1×10^{-3} s^{-1})

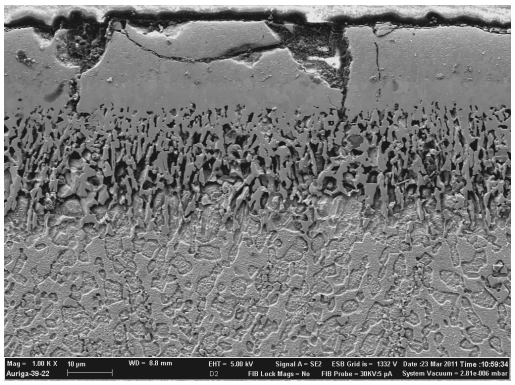

(b) Sample F (2×10^{-4} s^{-1})

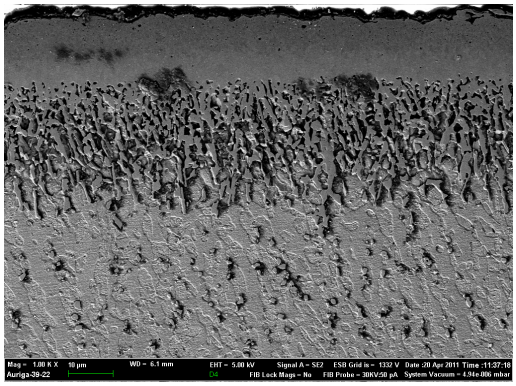

(c) Sample G (6×10^{-5} s^{-1})

Figure 4.13 FESEM images of boronized treated-DSS deformed at 1223 K for different strain rate; 1×10^{-3} s^{-1} (Sample E), 2×10^{-4} s^{-1} (Sample F) and 6×10^{-5} s^{-1} (Sample G) and strain of 0.4

From these results, it showed that when forming using superplastic material (treated-DSS), the hard boronized layer is able to withstand the load applied without cracks and produced low flow stress. It is important to notice that in order to be able to form surface hardened material without compromising on the surface disintegration, the flow stress during forming must be kept as low as possible. This could be achieved through the control of boronizing and heat forming parameters with the exploitation of superplastic deformation process.

CHAPTER 5

CONCLUSIONS

5.1 Conclusions

In this study, the effects of microstructure, strain rate and surface hardness on the forming process of the boronized treated-DSS were investigated. Characterizations on surface hardness, boronized layer and flow stress behaviour of the samples were done. Depending on boronizing time, boronized layer thickness of treated-DSS varied from 24 to 43 μm and surface hardness formed was in the range of 1890 to 2418 HV. Long duration time leads to the increment of boronized layer thickness and surface hardness. Boronized as-received DSS possesses a surface hardness and a boronized layer thickness of 2130 HV and 39 μm respectively.

For different surface hardness of boronized treated-DSS, the flow stress of high temperature forming was varied from 47 to 68 MPa. The flow stress is also increased as the hardness increases. Depending on types of microstructure, boronized treated-DSS produced lower flow stress as compared to boronized as-received DSS.

From the study, the following conclusions also can be made:

1. The flow stress during the forming process is strongly dependent on the surface hardness of the boronized layer, strain rate and initial microstructure conditions of the substrate.
2. Through superplasticity, the flow stress of the surface hardened sample can be kept or maintained as low as possible without creating any sign of surface disintegration.

5.2 Recommendations

Some suggestions for further study and development through the findings are stated as follows:

- The microstructure characterization such as EPMA analysis can be look into to evaluate the boron content of boronized samples.
- Mechanical testing such as wear test should be studied to investigate the product's performance.
- The processing techniques using different dimension of jigs and dies to form a product or parts
- The application using the results produced and its potential usage in the industry such as formation gear.

REFERENCES

Arieli, A., Mukherjee, A.K., (1980). A model for the rate-controlling mechanism in superplasticity. *Materials Science and Engineering*. **45 (1)**, *61-70*

Balokhonov, R.R., Stefanov, Yu.P., Makarov, P.V., Smolin, I.Yu., (2000). Deformation and fracture of surface-hardened materials at meso- and macroscale levels. *Theoretical and Applied Fracture Mechanic.* **33**, 9-15

Bloor, D., Brook, R.J., Flenings, M.C., Mahgan, S., (1994). The encyclopedia of advanced materials., Vol 4, Elsevier Science Ltd., Pergamon, UK., 2712-2722

Cabrera, J.M., Mateo, A., Llanes, L., Prado, J.M., Anglada, M., (2003). Hot deformation of duplex stainless steels. *Journal of Materials Processing Technology.* **143-144**, 321-325

Carrino, L., Giuliano, G., Polini, W., (2003). A method to characterize superplastic materials in comparison with alternative methods. *Journal of Materials Processing Technology*. **138**, 417 – 422

Chandra, N., (2002). Constitutive behavior of superplastic materials. *International Journal of Non-Linear Mechanics*. **37**,461-484

Friedman, P.A., Luckey, S.G., (2004). On the expanded usage of superplastic forming of aluminium sheet for automotive applications. *Material Science Forum*. **447-448**, 199-204

Gifkins, R.C., (1976). Grain-boundary sliding and its accommodation during creep and superplasticity. *Met. Trans.* **7**, 1225-1232

Han, Y.S., Hong, S.H., (1997). The effects of thermo-mechanical treatments on superplasticity of Fe-24Cr-7Ni-3Mo-0.14N duplex stainless steel. *Scripta Materialia*, **36 (5),** 557-563

Hasan, R., (2005). Development of superplastic boronizing using duplex stainless steel, Master Sc. Eng. Thesis, University of Malaya, Kuala Lumpur, Malaysia.

Henrik, S., Rolf, S., (2006). Fracture toughness of a welded duplex stainless steel. *Engineering Fracture Mechanics*. **73**, 377-90

Hertzberg, R.W., (1996). Deformation and Fracture Mechanics of Engineering Materials, 4th edn. New York: John Wiley & Sons.

Hoffmann, B., Vo¨hringer, O., Macherauch, E., (2001). Effect of compressive plastic deformation on mean lattice strains, dislocation densities and flow stresses of martensitically hardened steels. *Materials Science and Engineering A*. **319–321**, 299–303

Jauhari, I., Ogiyama, H., Tsukuda, H., (2002). Superplastic Diffusion Bonding of Duplex Stainless Steel. *Proceedings of 2nd. World Engineering Congress*, 22-25

Jiménez, J.A., Frommeyer, G., Carsí, M., Ruano, O. A., (2001). Superplastic properties of a δ/γ stainless steel. *Materials Science and Engineering A*. **307**, 134-142

Keddam, M., Chentaouf, S.M., (2005). A diffusion model for describing the bilayer growth (FeB/Fe_2B) during the iron powder-pack boriding. *Applied Surface Science*. **252 (2)**, 393-399

Kirthi, B., (2007). An approach to inverse modeling through the integration of artificial neural networks and genetic algorithms, Master Sc. in Mechanical Engineering Thesis, University of Kentucky, United States of America

Kohser, R.A., DeGarmo, E.P., Black, J.T., & Klamecki, B.E., (2003). Materials and Process in Manufacturing 8th edition, John Wiley & Sons, 134

Kum, D.W., Oyama, T., Sherby, O.D., Ruano, O.A., Wadsworth, J., (1984). In S.P. Agrawal (ed.) Superplastic Forming. American Society for Metals, Metals Park, 32.

Langdon, T.G., (1970). Grain boundary sliding as a deformation mechanism during creep. *Philosophical Magazine.* **22**, 689-700

Lutfullin, R.Y., Imayev, R.M., Kaibyshev, O.A., Hismatullin, F.N., Imayev V.M., (1995). Superplasticity and solid state bonding of the TiAl intermetallic compound with micro and submicrocrystalline structure. *Scripta Metallurgica et Materialia*. **33**, **9**, 1445-1449

Meric C., Sahin S., Yilmaz S.S., (2000). Investigation of the effect on boride layer of powder particle size used in boronizing with solid boron-yielding substances. *Materials Research Bulletin*. **35**, 2165-2172

Miyamoto, H., Mimaki, T., Hashimoto, S. (2001). Superplastic deformation of micro-specimens of duplex stainless steel. *Materials Science Engineering A*. **319-321**, *779-783*

Mohd Yusof H. A., (2010). Superplastic Boronizing of Duplex Stainless Steel through Dual Compression Method, Masters Sc. Eng. Thesis, University of Malaya, Kuala Lumpur, Malaysia.

Mukherjee, A.K., (2002). An examinationof the constitutive equation for elevated temperature plasticity. *Materials Science and Engineering A*. **322 (1-2)**, *1-22*

Mukherjee, A.K., (1971). The rate controlling mechanism in superplasticity. *Materials Science and Engineering*. **8 (2)**, *83-89*

Muthupandi, V., Bala Srinivasan, P., Seshadri, S. K., and Sundaresan, S., Shankar, V., (2005). Effect of nickel and nitrogen addition on the microstructure and mechanical properties of power beam processed duplex stainless steel (UNS 31803) weld metals. *Materials Letters*. **59**, 2305-2309

Ozbek, I., Konduk, B.A., Bindal, C., Zeytin, S., Ucisik, A.H., (2002). Characterization of borided AISI 316L stainless steel implant. *Vacuum*. **65**, *521-525*

Sinha A.K., (1991). Boronizing, ASM Handbook, OH, USA. *Journal of Heat Treatment*. **4**, 437-447

Superform Metals Limited (Eds.). (1988). Superplastic Aluminium Forming, Gulliver Press Ltd., United Kingdom

Tsuzuka, T., Takahashi, A., and Sakamoto, A., (1991). Application of superplastic forming for aerospace components, In Hori, S., Tokizane, M. and Furushiro, N. (eds). *Superplasticity in Advanced Materials*, 611-620

Tsuzaki, K., Xiaoxu, H., Maki, T., (1996). Mechanism of dynamic continuous recrystallization during superplastic deformation in a microduplex stainless steel. *Acta Metallurgica.* **44 (11)**, *4491-4499*

Valiev, R. Z., (2000). Superplastic Behaviour of Micro-and Nanograined Materials. *NATO Science Series*, **367**, 491-506

Vipin, J., Sundararajan, G., (2002). Influence of the pack thickness of the boronizing mixture on the boriding of steel. *Surface and Coatings Technology*. **149**, 21–26

Walser, B., Ritter, U., (1985). In B. Bandelet and M. Suery (eds.) Superplastic Centre National de la Recheache Scientifique, Paris, 15

Xing, H.L., Wang, C.W., Zhang, K.F., Wang, Z.R, (2004). Recent Development in the Mechanics of Superplasticity and Its Applications. *Journal of Materials Processing Technology*. **151**, 196-202

Xu. C. H., Xi J. K., and Gao W., (1997). Isothermal superplastic boronizing of high carbon and low alloy steels. *Scripta Maerialia*. **34 (3)**, *455-461*

Xun, Y.W., Tan, M.J., (2000). Applications of superplastic forming and diffusion bonding to hollow engines blades. *Journal of Materials processing Technology*. **99**, 80-85

Xu, C. H, Xi, J.K, and Gao, W. (1996), Isothermal superplastic boronizing of high carbon steel and low alloy steels. *Scripta Materialia.* **34(3).** 455-461

Yusof, H.A.M., Jauhari I., Saidan, R., (2011). Superplastic boronizing of duplex stainless steel under dual compression method. *Materials Science and engineering A*. **528**, 8106-8110

Zainul, H., (2004). Optical Microscopy, *A 2-Day Short Course on Materials Analysis, Characterization and Evaluation*, University of Malaya, Kuala Lumpur, Malaysia.

Zelin, M.G., Mukherjee, A.K., (1996). Geometrical aspects of superplastic flow. *Materials Science and Engineering A*. **208,** *210-225*

Zucchi, F., Grassi, V., Monticelli, C., Trabanelli, G., (2006). Hydrogen embrittlement of duplex
stainless steel under cathodic protection in acidic artificial sea water in the presence of sulphide ion. *Corrosion Science*. **48**, 522–530

INTERNET REFERENCES

URL: 1) http://www.metalwebnews.com/howto/superplastic-forming/superplastic-forming.html

URL: 2) http://www.nap.edu/html/materials_and_man/0309036976/HTML

URL: 3) http://www.asminternational.org/asmenterprise

URL: 4) http://www.lapump.com/html/duplex_stainless steel.html

PUBLICATIONS

Journal

I. Jauhari, H.A.M Yusof and **R. Saidan**. Superplastic boronizing of duplex stainless steel under dual compression method. Materials Science and Engineering A. Vols. 528 (2011) pp. 8106-8110.

R. Saidan and I. Jauhari. A Study on the High Temperature Forming Effect of Boronized Duplex Stainless Steel. (In-review in Journal of Materials Processing Technology)

Conference

R. Saidan and I. Jauhari. (2012) Effect of Superplastic Forming on Boronized Duplex Stainless Steel. Proceeding of 6th International Conference on Advanced Computational Engineering and Experimenting (ACEX-2012). 1-4 July 2012. Istanbul, Turkey.